Aus der Klinik für Neurologie mit Experimenteller Neurologie der
Medizinischen Fakultät Charité – Universitätsmedizin Berlin

DISSERTATION

# Effects of psychosocial stress on vascular function

zur Erlangung des akademischen Grades
Doctor of Philosophy (PhD)
im Rahmen des
International Graduate Program Medical Neurosciences

vorgelegt der Medizinischen Fakultät
Charité – Universitätsmedizin Berlin

von

Stephanie Wegner
aus Bernau bei Berlin

Datum der Promotion: 03.12.2021

*“Equipped with his five senses, man explores the universe around him and calls the adventure Science.”*

*Edwin Powell Hubble*

*The exploration of space. Harper's Magazine 158: 732-38. May 1929.*

## Preface

The thesis “Effects of psychosocial stress on vascular function” is based on the publication “Endothelial Cell-Specific Transcriptome Reveals Signature of Chronic Stress Related to Worse Outcome After Mild Transient Brain Ischemia in Mice” (**Wegner S**, Uhlemann R, Boujon V, Ersoy B, Endres M, Kronenberg G, Gertz K. Mol Neurobiol. 2020; 57(3): 1446-1458). This publication is licensed under a Creative Commons Attribution 4.0 International license (CC BY 4.0) (https://creativecommons.org/licenses/by/4.0/).

All results of the presented thesis have been published in the above mentioned publication.

My detailed contribution to the publication can be found on page 39 “Declaration of contribution”.

## Table of contents

## Abstract (English)

Chronic psychosocial stress is a risk factor for cardio- and cerebrovascular diseases. Human and animal studies show that chronic stress impairs endothelial function and worsens stroke outcome. However, the underlying molecular mechanisms still need to be elucidated. Therefore, the aim of this thesis was to identify chronic stress-associated endothelial mechanisms influencing stroke outcome.

To induce chronic psychosocial stress, wild-type 129S6/SvEv mice were at first exposed to a stress model over a course of 28 days. Then for induction of ischemic stroke, control (C) and chronically stressed (CS) animals were subjected to transient, 30-minute occlusion of the left middle cerebral artery, followed by reperfusion (30 min MCAo/reperfusion). At 48 h after stroke induction, lesion volume was measured by T2-weighted magnetic resonance imaging (MRI). Furthermore, after 72 h, cerebral endothelial cells (ECs) were isolated from infarcted and corresponding non-infarcted brain tissue from the contralateral hemisphere. In ECs, the differential gene expression was analyzed with RNA-sequencing (RNA-seq).

The applied chronic stress paradigm led to hyperactivation of the hypothalamic-pituitary-adrenal (HPA) axis with enlarged adrenal glands, increased FK506-binding protein 5 (FKBP5) expression in hypothalamus, and reduced weight gain. However, probably due to adaption of the stress axis, reduced levels of corticosterone were measured in plasma of CS compared to C mice after completion of the stress paradigm. CS mice displayed increased lesion sizes at 48 h after MCAo/reperfusion. Gene expression analyses with RNA-seq revealed a higher number of differentially expressed genes (DEGs) in ECs of CS versus C mice when the ipsilateral was compared with contralateral side. In CS mice, the DEGs were associated with biological processes, including proliferation, cell death, and neovascularization which are known to modulate stroke outcome. One of the detected DEGs in CS animals was microRNA (miR)-34a, which is associated with a reduced functional recovery after myocardial infarction, increased cell death, and reduced angiogenesis. In ischemic whole brain tissue, the expression of the mature microRNAs miR-34a-3p and miR-34a-5p correlated positively with the cerebral lesion size. In contrast, both microRNAs correlated negatively with the mRNA expression of the anti-apoptotic and

proliferation-promoting miR-34a target molecule sirtuin 1 (*Sirt1*) in ischemic brain tissue.

In summary, these results confirm that chronic psychosocial stress affects transcriptomic profile of ECs after ischemic stroke and leads to impaired stroke outcome. The increased miR-34a expression indicates stress-induced inhibition of regenerative processes, such as endothelial proliferation or angiogenesis, and increased cell death as mechanistic approach.

## Abstract (German)

Chronischer psychosozialer Stress gilt als Risikofaktor für kardio- und zerebrovaskuläre Erkrankungen. Humane und tierexperimentelle Studien zeigen, dass chronischer Stress zu einer gestörten Endothelfunktion führt und das Schlaganfallergebnis verschlechtert. Die zugrunde liegenden molekularen Mechanismen sind jedoch bis *dato* nicht ausreichend verstanden. Ziel dieser Arbeit war es daher endotheliale Mechanismen zu identifizieren, durch welche chronischer Stress das Schlaganfallergebnis beeinflusst.

Zunächst wurden 129S6/SvEv-Wildtypmäuse für 28 Tage einem Modell zur Induktion von chronischem psychosozialen Stress ausgesetzt. Anschließend erfolgte sowohl bei den Kontrolltieren als auch bei den chronisch gestressten Tieren die Induktion des ischämischen Schlaganfalls durch einen transienten, 30-minütigen Verschluss der linken *Arteria cerebri media* gefolgt von einer Reperfusion (30 min MCAo/ Reperfusion). Am Zeitpunkt 48 h nach MCAo/Reperfusion wurde die zerebrale Läsionsgröße mittels T2-gewichteter Magnetresonanztomographie (MRT) gemessen. Darüber hinaus wurden am Zeitpunkt 72 h zerebrale Endothelzellen sowohl aus dem infarzierten als auch aus dem korrespondierenden nicht-infarzierten Hirngewebe der kontralateralen Seite isoliert. Die differenzielle Genexpression wurde mittels RNA-Sequenzierung in den Endothelzellen analysiert.

Das eingesetzte chronische Stressparadigma führte zu einer Hyperaktivierung der Hypothalamus-Hypophysen-Nebennieren-Achse mit vergrößerten Nebennieren, einer erhöhten FK506-*binding protein* 5 (FKBP5)-Expression im Hypothalamus sowie einer verringerten Gewichtszunahme. Nach Beendigung des Stressparadigmas wurden jedoch im Plasma der chronisch gestressten Tiere niedrigere Corticosteronwerte als in der Kontrollgruppe detektiert, was wahrscheinlich durch eine Adaption der Stressachse bedingt ist. Vergleichen mit den Kontrolltieren besaßen die chronisch gestressten Mäuse 48 h nach MCAo/Reperfusion größere Hirninfarkte. Die Genexpressionsanalysen mittels RNA-Sequenzierung ergaben in den Endothelzellen der chronisch gestressten Mäuse verglichen mit den Kontrolltieren eine erhöhte Anzahl an differentiell exprimierten Genen beim Vergleich der ipsilateralen mit der kontralateralen Seite. In den chronisch gestressten Tieren waren diese Gene mit biologischen Prozessen wie Proliferation, Zelltod und Neovaskularisation assoziiert,

die bekanntermaßen das Schlaganfallergebnis modulieren. Als eines dieser in den gestressten Tieren differentiell exprimierten Gene wurde die MicroRNA (miR)-34a identifiziert, deren Expression mit verschlechterter funktionaler Regeneration nach einem Herzinfarkt, vermehrtem Zelltod und verminderter Angiogenese einhergeht. Untersuchungen im Schlaganfallgewebe zeigten eine positive Korrelation der reifen Sequenzen miR-34a-3p und miR-34a-5p mit der zerebralen Läsionsgröße. Im Gegensatz dazu korrelierten beide MicroRNAs negativ mit der mRNA-Expression des anti-apoptotisch wirkenden und proliferationsfördernden miR-34a-Zielmoleküls Sirtuin 1 (*Sirt1*) im ischämischen Ganzhirngewebe.

Zusammenfassend bestätigen diese Ergebnisse, dass chronischer psychosozialer Stress das endotheliale Transkriptionsprofil nach ischämischem Schlaganfall beeinflusst und zu einem verschlechterten Schlaganfallergebnis führt. Die verstärkte miR-34a-Expression weist hierbei auf eine stressvermittelte Inhibition regenerativer Prozesse wie endotheliale Proliferation bzw. Angiogenese und vermehrten Zelltod als mechanistischem Ansatz hin.

# 1. Introduction

## 1.1 Stress and stroke

Stroke was reported to be the second leading cause of death worldwide in 2016 [1]. Stroke etiology can be categorized into two major types: ischemic and hemorrhagic. Ischemic stroke results from vessel occlusion leading to a reduced blood supply (and simultaneously a reduction in oxygen and nutrient supply) in parts of the brain. Hemorrhagic stroke occurs through vessel rupture and bleeding into the brain or subarachnoid space [2]. In 2016, estimated 9.6 million first-ever ischemic and 4.1 million first-ever hemorrhagic strokes occurred worldwide, while approximately 2.7 and 2.8 million people died from ischemic and hemorrhagic stroke, respectively [1].

Clinical investigations have demonstrated a connection between psychosocial stress and cardio- and cerebrovascular diseases. Besides well-known risk factors, such as hypertension, active smoking, and diabetes mellitus, psychosocial stress has also been identified as risk factor for cardio- and cerebrovascular diseases [3–5].

A 1981 human study suggests a positive correlation between stroke severity and the amount of stress load in patients without prior background of cardiovascular disorders [6]. Complementary to this, clinical investigations indicate that the perception of stress is linked to augmented risk to suffer fatal stroke [7,8]. Experiments demonstrate significantly increased lesion volume and cognitive deficit after ischemic stroke in mice that received pre-stroke stress [9–12]. In these animals, increased damage susceptibility seems to be caused at least partially by endothelial dysfunction which in turn indicates to be mediated via glucocorticoid receptor and increased heart rate [11,12].

Ischemic stroke is characterized by a tissue damage through excitotoxicity starting immediately after the onset of vessel occlusion, whereas other damage and repair mechanisms have priority at later stages [13]. Different studies suggest that post-stroke neurogenesis is participating in functional recovery after stroke [14,15], but vascular mechanisms, including post-stroke angiogenesis, have also been demonstrated to be key aspects for determining stroke outcome and long-term recovery [16–18]. Furthermore, it has been shown that post-stroke angiogenesis and neurogenesis seem to be associated with each other. Inhibition of angiogenesis leads to a reduction in the number of immature neurons in the peri-infarct area [19]. Thereby, endothelial cells (ECs) seem to supply trophic support for migration of subventricular zone-developed neuroblasts to the peri-infarct tissue where they are able to evolve into mature neurons and develop synapses [19,20].

### 1.2 Hypothalamic-pituitary-adrenal (HPA) axis

During stress, control to maintain and restore homeostasis occurs through the autonomic nervous system together with the HPA axis [21]. Experimental data show the involvement of the amygdala in the HPA axis activation. Lesions in amygdala can decrease adrenocorticotrophin (ACTH) and glucocorticoid secretion after stress exposure, while amygdala stimulation leads to HPA axis activation [22]. HPA axis response to stress is initiated by corticotropin-releasing hormone (CRH) and arginine vasopression (AVP) synthesizing neurons in the medial parvocellular division of the hypothalamic paraventricular nucleus (PVN), which release CRH and AVP into the hypophyseal portal system at the median eminence. Release of CRH and AVP stimulates synthesis of pro-opiomelanocortin (POMC) and subsequently synthesis of ACTH in the anterior pituitary. Afterwards, ACTH is liberated into the blood stream and stimulates synthesis of glucocorticoids (primary corticosterone in rodents, cortisol in humans) in the adrenal cortex followed by glucocorticoid secretion into the blood stream [22–25]. Termination of the activated HPA axis occurs at the level of hippocampus, hypothalamus, and pituitary [23]. Furthermore, investigations indicate stressor-specific involvement of the medial prefrontal cortex in the cessation of HPA axis response [26]. Termination of the activated HPA axis occurs through glucocorticoid negative feedback which can be divided into fast (via non-genomic actions of glucocorticoids) and delayed (i.e., due to genomic action of corticosteroid receptors after glucocorticoid binding) negative feedback [27,28].
The pulsatile secretion of glucocorticoids under basal, non-stressed circumstances underlies a circadian rhythm with highest levels at beginning of the active phase and subsequently constant decrease to nadir in the inactive or sleeping period [29].

### 1.3 Corticosteroid receptors

Secreted glucocorticoids are capable of binding to different corticosteroid receptors; so-called mineralocorticoid receptors (MR) and glucocorticoid receptors (GR). The MR and GR are ligand-dependent transcription factors, i.e., upon ligand binding, the receptor complex translocates from cytosol into the nucleus, afterwards receptors dimerize either as homo- or heterodimer (e.g., MR and GR), and modulate gene expression [30–33]. Instead of modulating transcription through direct DNA binding, GR can also modulate gene expression through interference with different transcription factors [31]. Additionally, involvement of membrane-localized MR and GR in mediation of fast gene expression-independent corticosteroid effects has been described as well [28,34].

Investigations on rat brains suggest widespread expression of both receptors [35,36]. MR's affinity for corticosterone is approximately 6-10 times higher as compared to GR [37], whereas MR seems to have a similar affinity for aldosterone and the glucocorticoids cortisol and corticosterone [38,39]. However, due to the low aldosterone level compared to glucocorticoid concentration, MR is thought to bind particularly glucocorticoids in most brain areas [40]. Based on the distinct affinities of GR and MR, both receptors are differently occupied with hormones during day and after stress situations. Investigations on hippocampal samples from rats show MR occupation rate of approximately 90% either during peak phase of the circadian glucocorticoid rhythm or during morning trough, whereas GR is only occupied by 10% in the morning. After stress exposure, MR is nearly fully occupied while GR is around 70% occupied after restraint stress and during peak phase of the circadian rhythm [37]. MR seems to regulate basal activity of the HPA axis, whereas MR and GR together have demonstrated to mediate the negative feedback of the HPA axis during circadian glucocorticoid peak or after stress exposure [41,42]. A reduced negative feedback leads to prolonged activation of the HPA axis and prolonged activation has been indicated in psychiatric disorders like major depression where impaired GR-mediated negative feedback has been under extensive research [43].

### 1.4 FK506-binding protein 4 and 5 (FKBP4 and FKBP5)

FKBP4 and 5, also known as FKBP51 and FKBP52, are FK506-binding immunophilins, which can associate with steroid receptors, such as GR and MR [44–46]. FKBP5 can modulate transcriptional activity of steroid receptors differently between steroid receptor family members [46–49] but only the interaction between GR, FKBP4 and 5 is briefly discussed in the following.

Upon ligand binding on GR, an exchange between FKBP5 and FKBP4 has been described. If no ligand is in place FKBP5 is bound to GR complex, otherwise after glucocorticoid exposure, FKBP5 gets replaced by FKBP4 and the whole complex translocates into the nucleus where receptor modulates gene transcription [31,50]. Thereby, FKBP4 promotes the nuclear translocation through direct interaction with dynein [47,51,52]. FKBP5 has been demonstrated to reduce the affinity of GR for ligand binding and to diminish translocation of GR into the nucleus [47,53,54]. Interestingly, *in vivo* as well as *in vitro FKBP5* mRNA expression becomes strongly upregulated after stimulation with glucocorticoids via GR-mediated transcription and the increased FKBP5 expression provides therefore an intracellular short negative feedback mechanism of the glucocorticoid signaling [55,56]. In New World monkeys, it has been demonstrated that FKBP5 overexpression provokes glucocorticoid resistance, which in turn is counteracted by increased cortisol levels in these animals [57,58]. The importance of basal FKBP5 expression in regulation of GR sensitivity was further illustrated in mice where a strong stressor, like food deprivation, leads to *Fkbp5* mRNA upregulation in different regions all over the brain but with highest induction in areas with low basal *Fkbp5* expression. Whereas a lower stressor seems to raise *Fkbp5* expression only in areas with a low basal expression, like the PVN in the hypothalamus, but not in regions with strong basal *Fkbp5* level, like the hippocampus, probably due to higher glucocorticoid resistance in these tissues [59].

In human brain, an increase in FKBP5 expression with increasing age has been described [60]. Lately, it has been proposed that age- and stress-associated upregulation of *FKBP5* in immune cells can stimulate inflammation and could therefore promote the development of cardiovascular diseases [61].

Designated alleles of the *FKBP5* polymorphisms indicate a connection with diminished recovery in cortisol levels and an enhanced anxiety level after psychosocial stress exposure. Bearing these alleles might comprise a risk factor for development of stress-associated diseases after repeated stress [62].

## 1.5 MicroRNA-34a (miR-34a)

MicroRNAs (miRNAs) are about 22 nucleotides long non-coding RNAs that negatively regulate gene expression at post-transcriptional level either due to mRNA degradation or protein translation inhibition [63–65]. MicroRNA maturation starts in the nucleus where protein Drosha cuts the primary miRNA into approximately 70 nucleotides long precursor miRNA (pre-miRNA). The pre-miRNA is transported with the assistance of Exportin-5 into the cytoplasm, where Dicer trims the pre-miRNA into approximately 22 nucleotide long mature miRNA [66–70]. The mature miRNA becomes integrated into RNA-induced silencing complex (RISC) and navigates the complex to specific mRNA targets [71–73]. One microRNA can have different mRNA-targets and one mRNA can be regulated by different miRNAs [63,74].

In mice, highest expression of miR-34a was detected in the brain, followed by lung, heart, and kidney [75]. Age-increased miR-34a expression has been demonstrated for instance in the brain, heart, aorta, spleen, and bone marrow-derived mononuclear cells in humans and/or mice [76–80].

Few days after acute myocardial infarction in mice, an increase in miR-34a expression was detected within the ischemic boundary area and inhibition of miR-34a leads to increased vessel density, decreases cell death, and enhances cardiac function [77]. Naturally in the mouse heart, miR-34a expression increases sharply within the first few days after birth and *in vivo* experiments suggest that the heart's ability to regenerate after myocardial infarction is prevented with increased expression of miR-34a [81].

In human umbilical vein endothelial cells (HUVECs), miR-34a inhibits angiogenic sprouting and promotes cellular senescence [77,78]. It has been demonstrated that miR-34a inhibits endothelial cell proliferation due to cell cycle arrest in G1 phase [78]. Furthermore, *in vitro* experiments suggest increased permeability of blood-brain barrier as a result of miR-34a overexpression in endothelial cells [82].

The expression of the deacetylase SIRT1 has been demonstrated to be repressed by miR-34a [78,83]. SIRT1 appears to regulate hypoxic and oxidative stress response, survival, and angiogenesis for instance through deacetylation of the transcription factors p53, FOXO3, FOXO1, or HIF-2α [84–88]. It seems that miR-34a promotes cellular senescence and inhibits cell proliferation (at least to a certain degree) through the inhibition of SIRT1 expression in primary endothelial cells [78]. After treatment with

DNA-damaging agents, literature shows p53-induced increment of miR-34a expression [89–91]. Due to expression inhibition of the deacetylase SIRT1, miR-34a appears to increase p53 acetylation, which in turn activates the p53 signaling pathway. It is therefore proposed that a positive feedback loop between p53 and miR-34a via repression of SIRT1 expression exists [83].

Besides SIRT1, further miR-34a targets have been determined whose expression inhibition might be responsible for the detrimental effects of miR-34a as well [e.g., 77,92]

### 1.6 Motivation and aims of the thesis

Previous publications have indicated that stress-induced endothelial dysfunction contributes to increased lesion size after ischemic stroke [11,12]. Against this background, the overall objective of this thesis was to investigate and characterize the transcriptomic profile of ECs after chronic stress and stroke exposure in order to reveal potential cellular targets and mechanisms associated with the detrimental effects of pre-stroke chronic stress on stroke outcome.

Effects of stress are certainly not limited to one cell type in the brain. For example, it seems that even acute stress events could reduce proliferation of precursors cells which in turn may affect functional outcome after stroke [14,93]. Chronic stress and glucocorticoid treatment seem to be able to change morphology and numbers of neurons, respectively [94,95]. Furthermore, literature suggests that stress could lead to an activated microglia phenotype [96,97]. However, the focus of transcriptomic analysis was placed on ECs because vascular mechanisms have been shown to be key aspects for determining the outcome of stroke [16,17,98].

Moreover, this thesis aims at characterizing the dysregulation of the HPA axis after chronic stress procedure by investigating gene and protein expression related to corticosteroid signaling in the hypothalamus - an essential structure for initiating HPA axis responses and important for negative feedback [22,23]. Special emphasis was laid on the FKBP5 mRNA and protein expression as a feasible marker to evaluate glucocorticoid level and regulator of GR sensitivity [53,55,59].

# 2. Materials and methods

A profound description of all materials and methods is given in publication itself. In this chapter only pivotal material and methods are delineated.

## 2.1 Animals

All animal experiments were permitted by the responsible authority (Landesamt für Gesundheit und Soziales, Berlin, Germany) under license number G 0167/15. Wild-type male 129S6/SvEv mice were bred by the "Forschungseinrichtungen für Experimentelle Medizin" (FEM) of the Charité - Universitätsmedizin Berlin and were approximately 8-10 weeks old at the beginning of the stress procedure. For the stressor "exposure to rat", approximately 9-11 weeks old male Wistar rats purchased from Charles River Laboratories were used. Mice and rats were kept in standard cages equipped with a house, nesting material, and for rats wooden blocks. Animals lived in regulated environment with following characteristics: temperature: 22 °C ± 2 °C; humidity: 55% ±10%; 12:12 h light-dark cycle. Lights were turned on at 6:00 a.m. All animals had *ad libitum* access to food and water.

## 2.2 Chronic stress procedure

The chronic stress paradigm, developed by Strekalova *et al.* [99], consisted of three different stressors, i.e., exposure to rat, restraint stress, and tail suspension, which were performed in the following order: days 1-7 exposure to rat, days 8-10 restraint stress, days 11-17 exposure to rat, days 18-22 tail suspension, days 23-25 restraint stress, days 26-28 tail suspension.

<u>Exposure to rat</u>

One single mouse was placed inside a small cage (dimensions: height 140 mm x width 167 mm x length 252 mm) which in turn was placed inside a rat cage (dimensions: height 200 mm x width 375 mm x length 585 mm) with one rat. Mice were exposed to rats for 15 h (6 p.m. to 9 a.m.). During the procedure, all animals had *ad libitum* access to food and water. A single exposure to rat for 15 h has also been used as acute stress model.

Restraint stress

To allow air and heat exchange during the procedure, the needle adapter of 50 mL syringe (Omnifix® Solo 50 mL, B. Braun Melsungen AG) was removed beforehand. During the dark phase, each mouse was placed inside a syringe for 1 h (7 p.m. to 8 p.m.) to induce restraint stress.

Tail suspension

At 7 p.m., mice were suspended by the tail for 6 min per day. The procedure was conducted by hand from the height of 80 cm approximately.

## 2.3 Middle cerebral artery occlusion (MCAo)

For induction of the cerebral ischemia in mice, the established procedure described in "Standard operating procedures (SOP) in experimental stroke research: SOP for middle cerebral artery occlusion in the mouse" [100] was used.

In short, mice were initially anaesthetized with 1.5% isoflurane in 69% $N_2O$ and 30% $O_2$. During surgery, isoflurane was reduced to 1.0%. A silicone resin/hardener mixture (Xantopren M Mucosa and Activator NF Optosil Xantopren, Heraeus Kulzer GmbH) coated 8.0 nylon monofilament was inserted into the left common carotid artery, advanced into the left internal carotid artery until reaching the anterior cerebral artery. After 30 min of middle cerebral artery and anterior choroidal artery occlusion, the filament was removed to enable reperfusion. During surgery and occlusion, body temperature was kept constant at 36.5 ± 0.5 °C using heating pad and box, respectively. Afterwards, mice were kept at 36.5 ± 0.5 °C for additional 2 h.

## 2.4 Magnetic resonance imaging (MRI)

Two days after surgery, MRI was used to verify successful MCAo. MRI was conducted with a 7 Tesla rodent scanner (PharmaScan® 70/16, Bruker Corp.) and 20-mm $^1$H-RF quadrature-volume resonator. Lesion volume was assessed using T2-weighted two-dimensional turbo spin-echo sequence (imaging parameters: repetition time/echo time (TR/TE) = 4200/36 ms, rare factor 8, 4 averages, 32 axial slices with 0.5 mm thickness each, field of view: 2.56 × 2.56 cm, matrix size: 256 × 256). During scan, mice were anaesthetized using 1-2% isoflurane in 70% $N_2O$ and 30% $O_2$ and the respiratory rate was observed with a small animal monitoring and gating system (SA Instruments, Inc.). Lesion size was determined with the software Analyze 10.0 (AnalyzeDirect, Inc.) and edema-corrected with the equation as reported by Gerriets *et al.* [101].

## 2.5 Isolation of brain ECs

Three days after MCAo, transcardial perfusion with 0.9% saline was performed with control (C) and chronically stressed (CS) animals. After rapid brain removal, the brain tissue from the ipsilateral hemisphere (i.e., middle cerebral artery (MCA) territory) and the corresponding contralateral area (i.e., comparable non-infarcted tissue from the other hemisphere) were isolated and stored separately in 4 °C cold PBS (without $Ca^{2+}$ & $Mg^{2+}$). Firstly, per RNA-sequencing (RNA-seq) sample brain tissue from 3-5 animals was pooled and dissected with Neural Tissue Dissociation Kit (P) according to manufacturer's manual protocol (Miltenyi Biotec GmbH). In addition, Buffer X was prepared with the stated amount of β-mercaptoethanol beforehand. The obtained brain tissues were washed once with cold Hanks' Balanced Salt Solution (HBSS, without $Ca^{2+}$ & $Mg^{2+}$) before the enzyme mix 1 solution was added. After cell suspension filtration using cell strainer with 70 µm of mesh size, all following steps in the entire isolation procedure were either performed on ice or at 4 °C. Secondly, each sample was resuspended in 200 µl of Myelin Removal Beads II (Miltenyi Biotec GmbH) together with 1800 µl of buffer and the manual protocol was followed. Thirdly, cells were resuspended in 20 µl of CD31 MicroBeads and 180 µl buffer and the provided protocol from Miltenyi Biotec GmbH was used. CD31 positive cells were enriched in two repetitive steps with MS columns and the OctoMACS as separator. To guaranty high degree of endothelial cell purity, an extra FACS step was conducted. Therefore, cell suspension was incubated with antibodies against CD31, CD146, and CD45 for 10 min at 4 °C in FACS buffer (1x PBS with 0.5% BSA + 0.01% $NaN_3$). Afterwards, cells were washed twice and were resuspended in 150 µl FACS buffer. Shortly before sorting, 1.5 µl of DAPI stock solution (2 µg/ml) was added to the cell suspension.

CD45-/DAPI-/CD31+/CD146+ single cells were isolated using a BD FACSAria™ II flow cytometer and were used for RNA-seq. Following antibodies and dilutions were used for FACS staining: anti-mouse CD31-Alexa Fluor® 488 (#102514, BioLegend, Inc) 1:170; anti-mouse CD45-APC (#130-102-544, Miltenyi Biotec GmbH) 1:10; anti-mouse CD146 (LSEC)-PE (#130-102-319, Miltenyi Biotec GmbH) 1:10.

### 2.6 RNA-seq of isolated brain ECs

Total RNA from brain ECs was isolated with the NucleoSpin® RNA XS Kit according to the manufacturer's protocol (MACHEREY-NAGEL GmbH & Co. KG) but without the optional filtration step and usage of carrier RNA. RNA was eluted in 12 µl RNase-free water. LGC Genomics GmbH (Berlin, Germany) evaluated RNA quality with the Agilent 2100 Bioanalyzer (Agilent Technologies, Inc.), performed cDNA synthesis, library preparation with Encore Rapid DR Multiplex system (NuGen Technologies, Inc.), conducted the sequencing, performed data pre-processing, differential expression analysis, and principal component analysis (PCA). The libraries were sequenced on the Illumina® NextSeq™ 500 with 150 bp paired-end reads. In total, approximately 400 million read pairs were sequenced.

RNA-seq data are available at Gene Expression Omnibus (GEO) database under accession number GSE122345.

Investigation of differentially expressed genes (DEGs)

With STAR 2.4.1b [102], LGC Genomics GmbH aligned the reads to the reference genome *Mus musculus* (GRCm38; Ensembl version 84). After alignment, reads mapped to ribosomal and transfer RNA regions were removed and htseq-count was used for counting the aligned reads [103]. Using Cuffdiff 2.1.1, LGC Genomics GmbH computed the fragments per kilobase per million fragments mapped (FPKM) values and performed differential expression analysis. The Benjamini-Hochberg false discovery rate (FDR) method was applied to correct the initial *p*-values for multiple comparisons and genes with an FDR-adjusted $p$-value < 0.05 and fold change ≥ 2 or ≤ -2 were defined as DEGs. For some genes a log2(fold change) value of ±infinity was calculated because these genes could not be detected in ECs from ipsilateral or contralateral side. Genes with an FDR-adjusted $p$-value < 0.05 and log2(fold change) of ±infinity were not considered as differentially expressed due to the low mean read count of <4 in ECs from the opposite side of the brain. In C mice 5 genes (*Gm13755, Gm3191, Igkv4-58, Gm6064, 1700017I07Rik*) and in CS mice 2 genes (*Gm24447, Gm11686*) fell into this category.

Based on the FPKM values, the expression of different cell type-specific genes were illustrated with the tool Heatmapper [104]. The specific markers were collected from various publications [105–112]. The Venn diagram of DEGs was generated with InteractiVenn [113].

<u>Gene Ontology (GO) enrichment analysis</u>

DEGs detected between ipsilateral and contralateral ECs were used for the GO enrichment analysis with g:Profiler [114; Ensembl version 91]. The minimum and maximum size of functional categories were set to 5 and 5000 genes, respectively and the Benjamini-Hochberg FDR method was applied for multiple testing correction. Biological process GO terms were defined as significantly enriched if an FDR-adjusted $p$-value < 0.01 was calculated. To summarize biological process GO term lists, redundant GO terms were removed with REVIGO [115].

### 2.7 Statistics

To prevent bias, all procedures and analyses were conducted in a blinded manner with the exception of the stress experiments. Additionally, all mice were randomized to the experimental groups. GraphPad Prism version 7 or 8 (GraphPad Software, Inc.) was used for statistical analysis. Data was tested for normal distribution using D'Agostino-Pearson omnibus test (n ≥ 8) or Shapiro-Wilk test (n < 8). Depending on the number of independent groups, normally distributed data was analyzed with the unpaired t-test or the one-way Analysis of Variance (ANOVA) followed by Tukey's multiple comparison test. For two independent data sets with non-normal distribution, the Mann-Whitney U-Test was applied. In correlational studies depending on presence of normal distribution or not, the Pearson's or the Spearman's rank correlation coefficient was calculated. Results with $p$-value < 0.05 were considered as statistically significant. Mice with intracerebral hemorrhage (C: 0%, CS: 3%) or those who did not show successful MCAo (C: 19%, CS: 21%) were excluded from this study.

## 3. Results

At the end of the chronic stress procedure, CS animals revealed significantly reduced weight gain and significantly increased adrenal weight in comparison to C mice (Fig. 1b-d*). In the morning 12 hours after applying the last stressor, CS mice displayed significantly decreased corticosterone plasma levels in comparison to C mice, whereas acutely stressed (AS) animals showed significantly increased corticosterone values shortly after completion of the acute stress procedure (Fig. 1e*). On the left side of the hypothalamus, expression of the glucocorticoid receptor (*Nr3c1*), mineralocorticoid receptor (*Nr3c2*), and *Fkbp4* mRNA did not differentiate significantly between C and CS animals but *Fkbp5* and *Crh* mRNA expression were significantly upregulated in CS mice (Fig. 1f*). Furthermore, on the right side of the hypothalamus, significantly elevated FKBP5 protein expression was measured in CS mice compared to C animals as well (Fig. 1g, h*).

Overall, in comparison to C animals, significantly enlarged lesion volume was detected in CS mice two days after 30 min MCAo/reperfusion (Fig. 2b*). Three days after ischemia, ECs from the MCA territory and the corresponding contralateral tissue were isolated (Fig. 2c, d*) and analyzed with RNA-seq. The EC samples from C and CS animals showed strong expression of endothelial cell-specific markers, whereas marker genes of other brain cell types were very weakly expressed (Fig. 2e*). In the EC samples from the corresponding contralateral tissue, no DEGs were detected between C and CS mice. In Fig. 3 a, b*, the Volcano plots show the expression between ipsilateral and contralateral for all genes in ECs of the C and CS group. In comparison to C mice, a greater number of DEGs between ipsilateral and contralateral ECs was identified in CS animals (C: 149 DEGs; CS: 207 DEGs) (Fig. 3c*). An entire list of the C and CS animals detected DEGs can be found in the supplementary material ESM 2-4*. In total, 93 DEGs were identically regulated in both groups (Fig. 3c, ESM 2*). Analysis with the DEGs revealed biological process GO terms that were either concurrently enriched in C and CS animals, or solely enriched in CS or C mice (ESM 1a-c*). The DEGs of CS mice were linked to biological processes like proliferation, cell death, and neovascularization (Fig. 3e, ESM 1b*). The miR-34a was one of the upregulated DEGs in ECs from CS animals when the ipsilateral was

* All figures including supplementary material can be found in the attached publication.

compared with contralateral side (Fig. 3b*). This microRNA was assigned to nine out of the top 10 significantly enriched biological process GO terms in CS animals which are shown in Fig. 3e*.

For investigations in ischemic whole brain tissue, the CS group was separated into two groups because of inhomogeneity in lesion sizes; ‘CS large’ group with lesion volume higher and ‘CS small’ group lower than the median. In ischemic brain tissue, the ‘CS large’ group showed significantly elevated expression of the mature microRNAs miR-34a-5p and -3p and significantly reduced *Sirt1* mRNA expression in comparison to C animals and the ‘CS small’ group (Fig. 4a-c*). However, miR-34a-5p, miR-34a-3p, and *Sirt1* expression did not vary significantly between C and the ‘CS small’ group (Fig. 4a-c*). The *Fkbp5* expression between the C, ‘CS small’, and ‘CS large’ group were not significantly different in stroke-damaged tissue as well (Fig. 4d*). Overall, in ischemic whole brain tissue the expression of miRNA-34a-5p and -3p correlated moderately positively with MRI-determined lesion size and moderately negatively with *Sirt1* mRNA expression (Fig. 4f-i*). Whereas, *Sirt1* and *Fkbp5* mRNA expression in ischemic brain tissue were moderately negatively and positively correlated with infarct volume, respectively (Fig. 4e, j*).

---

* All figures including supplementary material can be found in the attached publication.

## 4. Discussion

Possibly depending on several determinants, such as age, strain, sex, type of stressor, and stress duration, different stress models have been shown to have a diverse effect on body weight in mice [99,116–120]. Previously, Strekalova *et al.* illustrated a decreased body weight in C57BL/6N mice after using the 28-day chronic stress model [99]. Here, in accordance with the results by Strekalova *et al.,* reduced weight gain was detected in chronically stressed 129S6/SvEv mice compared to littermate controls at the end of chronic stress procedure. Furthermore, enhanced adrenal weight and *Crh* expression (during the circadian glucocorticoid trough and approximately 12 hours after exposure to the last stressor) together with elevated FKBP5 expression in hypothalamus indicate depression-like hyperactivity of the HPA axis and glucocorticoid resistance in CS mice. In the present investigation only one regulatory brain region of the HPA axis was investigated. In the future it would be interesting to know if potential glucocorticoid resistance occurs as well in multiple regulatory regions.

The central administration of CRH can lead to depression-like changes in animals [121,122]. Additionally, in postmortem samples obtained from depressed patients, increased *CRH* mRNA expression level (compared with controls) has been detected in the PVN [123,124]. Unlike Wang *et al.* who detected increased *CRH,* as well as mineralocorticoid receptor (*NR3C2*) mRNA level in the PVN of depressive patients [123], no change was measured in *Nr3c2* expression between CS animals and control in whole hypothalamus tissue.

*FKBP5* expression has been described as feasible marker to evaluate glucocorticoid level because it is strongly induced after glucocorticoid exposure [55]. Moreover, increased FKBP5 expression has been demonstrated to provoke glucocorticoid resistance in New World monkeys [57,58]. In forced swim test, chronically stressed FKBP5 knockout mice show an enhanced active stress coping likely through augmented feedback inhibition in the HPA axis [125]. In the present study, no behavioral analyses have been performed. Therefore, it cannot be ruled out that CS mice did not develop depressive-like phenotype, despite the above-mentioned molecular findings.

Surprisingly, mice that were exposed to the acute stress model had elevated plasma corticosterone level in the morning, whereas CS animals had reduced level at the end.

Reduced corticosterone after completion of chronic social defeat paradigm has been recorded as well by Savignac *et al.* [118]. That group also took the corticosterone samples the day after completion of chronic stress procedure and, according to its authors, the reduction in corticosterone level possibly displays adaptive alteration of the HPA axis to chronic stress [118].

In rats, reduction in GR expression on mRNA level in the PVN has been described after chronic stress [126,127]. A change in hypothalamic GR expression of CS mice was neither observed on mRNA nor on protein level in the present investigation. Besides a difference in mRNA expression, a change in the phosphorylation status of GR has also been reported after stress exposure in hippocampus and prefrontal cortex of both rats and mice [128,129] and it has been shown that GR phosphorylation can modulate for instance transcriptional activity of the receptor [130,131]. In the context of current study, it cannot be ruled out that changes in post-translational modifications of the GR in hypothalamus tissue may affect regulation of HPA axis.

In accordance with previously published studies [11,12], enlarged ischemic lesion volumes in CS mice were measured when using the 28-day chronic stress paradigm. But it must be acknowledged that neither the present investigation nor the previous published results from Balkaya *el al.* [11] or Custodis *et al.* [12] illustrate a direct relation between chronic stress and impaired functional outcome after MCAo/reperfusion. However, the analysis from Sugo *et al.* suggests that besides increased infarct volumes, cognitive function in pre-stroke stressed mice after MCAo/reperfusion is also impaired as compared to non-stressed animals [10].

Despite the significantly increased lesion volume in CS mice, a strong inhomogeneity in lesion size existed within this group, probably due to partly resilience to the detrimental stress effects. But based on investigations shown in Fig. 1, it appears unlikely that all mice with small lesion size were resilient to the stressors. Investigations illustrate that in the PVN, methylation of *Crh* gene possibly prevents the *Crh* induction in stress-resilient mice, whereas in susceptible mice, *Crh* expression seems to be elevated due to demethylation after chronic stress exposure [132]. Based on augmented *Crh* expression and alteration in other stress-related parameters like weight gain and adrenal weight, it appears that most 129S6/SvEv mice responded susceptibly to the used chronic stress procedure, but these animals (depicted in Fig. 1) were not used for stroke experiments. However, a high response rate to chronic stress and strong variance in lesion size within the CS group suggest that not all of stress-susceptible animals developed increased lesion size after ischemia. Some animals were probably partly resilient to the detrimental effects of chronic stress.

Coronary endothelial dysfunction is linked to elevated risk for cerebro- and cardiovascular incidents [133–135]. It has been suggested that stress-induced endothelial dysfunction could be the underlying cause for the augmented vascular risk in stress individuals [136,137]. Mechanistically, in animals it has also been indicated that chronic stress at least partially increases infarct size after MCAo/reperfusion through endothelial dysfunction. Thereby, endothelial dysfunction seems to be caused via GR signaling and increased heart rate [11,12], but EC-specific analysis after MCAo/reperfusion has not been performed thus far. Therefore, in the present study, the effects of pre-stroke chronic stress on brain ECs were investigated with RNA-seq in mice after ischemia.

Between contralateral EC samples from C and CS mice no DEGs were detected, whereas in previous investigations the 28-day chronic stress paradigm alone provoked endothelial dysfunction along with reduction in endothelial nitric oxide synthase (eNOS) expression [11,12]. Additionally, endothelial dysfunction after brief mental stress exposure has also been demonstrated in humans [138–140]. In current investigation, it is important to note that the ECs were isolated 72 h after stroke and approximately 84 h after last stressor exposure, whereas Balkaya *et al.* [11] or Custodis *et al.* [12] have determined endothelial function after termination of chronic stress procedure without ischemia. Endothelial dysfunction triggered by brief stress procedure has been demonstrated to remain only temporary [139,140]. Therefore, it is possible that the time frame between last stressor and sacrifice was too long to detect any differences in gene expression. Also noteworthy is the fact that the MCAo increases the circulating level of corticosterone [e.g., 141]. The MCAo procedure can therefore be considered as a strong stressor itself and may abrogated the transcriptomic differences in ECs from contralateral hemisphere between both groups at the time of sacrifice.

In C as well as CS group, only a low number of DEGs was detected between ipsilateral and contralateral ECs. All biological process GO terms enriched in C, CS or both groups are depicted in the supplementary material ESM 1. The top 10 of biological process GO terms only enriched in CS mice among others included “cell proliferation”, “negative regulation of biological process”, “positive regulation of apoptotic process”, “cell death”, “negative regulation of cell proliferation”, “circulatory system development”, and “cardiovascular development”. MiR-34a was detected as one of the upregulated DEGs between ipsilateral and contralateral ECs from CS animals and was assigned to nine out of the top 10 significantly enriched biological process GO terms.

In primary ECs, it has been demonstrated that miR-34a promotes cellular senescence and inhibits cell proliferation at least partially through inhibition of SIRT1 expression [78]. *In vitro* experiments indicate that miR-34a overexpression in endothelial cells could lead to increased permeability of blood-brain barrier [82]. Moreover, after acute myocardial infarction, inhibition of miR-34a increases vessel density in ischemic boundary area [77]. Altogether, these data propose adverse impact of miR-34a induction on endothelium. Based upon literature [83], it is hypothesized that chronic stress in combination with ischemic injury leads to post-translational modification of p53, such as acetylation which results in its enhanced transcriptional activity. The resulting miR-34a upregulation inhibits for instance proliferation and promotes apoptosis through repression of SIRT1 expression [78,83]. But further investigations are needed to confirm the role of endothelial miR-34a on stroke outcome. It would be important to analyze vessel density and cerebral blood flow in the ischemic striatum of C and CS animals to verify the obtained RNA-seq results. Neovascularization and increased cerebral blood flow have indicated to be crucial for stroke outcome [16,17,98].

For RNA-seq, the tissue from 3-5 animals were pooled for enough ECs. Therefore, no direct correlation between endothelial miR-34a expression and lesion size was feasible. Furthermore, each pre-miRNA consists of two arms and often out of each arm a mature miRNA can emerge, which is additionally labeled with 5p or 3p [142,143]. Consequently, in follow-up experiments, the expression of the mature microRNAs (i.e., miR-34a-5p and miR-34a-3p), *Sirt1*, and *Fkbp5* was investigated in ischemic brain tissue from CS and C mice. An obvious weakness of ischemic whole brain tissue investigation is that other cell types besides ECs may express miR-34a, as well [144–146]. Furthermore, other miR-34a targets besides SIRT1 exist whose expression inhibition might further mediate the effects of miR-34a [e.g., 77,92].

The current investigation in stroke-damaged tissue revealed a positive correlation between miR-34a-5p or miR-34a-3p expression and lesion size, whereas *Sirt1* was negatively correlated with the expression of both mature microRNAs and lesion volume. Literature contains evidences indicating a direct influence of miR-34a and SIRT1 expression on ischemic injury and outcome. For example inhibition of miR-34a has been shown to diminish cell death as well as fibrosis and to enhance the cardiac contractile function while its overexpression in regenerable neonatal hearts inhibits functional recovery after myocardial infarction [77,81]. In contrast, SIRT1 expression is suggested to have cardioprotective function against myocardial ischemia/ reperfusion; cardiac-specific overexpression appears to decline, whereas its knockout stimulates myocardial injury [147]. Furthermore, SIRT1 activates eNOS through deacetylation and, due to promotion of NO-dependent vascular relaxation, it is thought to be cerebrovascular protective after cerebral hypoperfusion [148]. A similar result has been suggested in hearts of diabetic rats where cardiac-specific SIRT1 overexpression decreased the myocardial ischemia/reperfusion injury, likely through increased eNOS activity [149].

Whereas the above mentioned results and literature indicate that miR-34a expression modulates lesion size, miR-34a mimics has been dealt as a promising anti-tumor agents but due to severe adverse reactions the clinical trial has been stopped earlier [150].

Overall, the present investigation supports the observation that chronic stress raises stroke vulnerability. After ischemia, the transcriptomic profile of ECs in chronically stressed mice is linked to poor stroke outcome and the miR-34a appears to be a key candidate molecule exacerbating brain injury.

## 5. References


1. GBD 2016 Stroke Collaborators. Global, regional, and national burden of stroke, 1990–2016: a systematic analysis for the Global Burden of Disease Study 2016. Lancet Neurol. 2019;18(5):439–58.

2. Rink C, Khanna S. Significance of brain tissue oxygenation and the arachidonic acid cascade in stroke. Antioxid Redox Signal. 2011;14(10):1889–1903.

3. Everson-Rose SA, Roetker NS, Lutsey PL, Kershaw KN, Longstreth Jr WT, Sacco RL, Diez Roux AV, Alonso A. Chronic stress, depressive symptoms, anger, hostility and risk of stroke and transient ischemic attack in the Multi-Ethnic Study of Atherosclerosis. Stroke. 2014;45(8):2318–23.

4. O'Donnell MJ, Xavier D, Liu L, Zhang H, Chin SL, Rao-Melacini P, Rangarajan S, Islam S, Pais P, McQueen MJ, Mondo C, Damasceno A, Lopez-Jaramillo P, Hankey GJ, Dans AL, Yusoff K, Truelsen T, Diener HC, Sacco RL, Ryglewicz D, Czlonkowska A, Weimar C, Wang X, Yusuf S, INTERSTROKE investigators. Risk factors for ischaemic and intracerebral haemorrhagic stroke in 22 countries (the INTERSTROKE study): a case-control study. Lancet. 2010;376(9735):112–23.

5. Rosengren A, Hawken S, Ounpuu S, Sliwa K, Zubaid M, Almahmeed WA, Blackett KN, Sitthi-amorn C, Sato H, Yusuf S, INTERHEART investigators. Association of psychosocial risk factors with risk of acute myocardial infarction in 11119 cases and 13648 controls from 52 countries (the INTERHEART study): case-control study. Lancet. 2004;364(9438):953–62.

6. Carasso R, Yehuda S, Ben-Uriah Y. Personality type, life events and sudden cerebrovascular attack. Int J Neurosci. 1981;14(3–4):223–5.

7. May M, McCarron P, Stansfeld S, Ben-Shlomo Y, Gallacher J, Yarnell J, Davey Smith G, Elwood P, Ebrahim S. Does psychological distress predict the risk of ischemic stroke and transient ischemic attack? The Caerphilly Study. Stroke. 2002;33(1):7–12.

8. Iso H, Date C, Yamamoto A, Toyoshima H, Tanabe N, Kikuchi S, Kondo T, Watanabe Y, Wada Y, Ishibashi T, Suzuki H, Koizumi A, Inaba Y, Tamakoshi A, Ohno Y, and JACC Study Group. Perceived mental stress and mortality from cardiovascular disease among Japanese men and women: the Japan Collaborative Cohort Study for evaluation of cancer risk sponsored by Monbusho (JACC Study). Circulation. 2002;106(10):1229–36.

9. DeVries AC, Joh HD, Bernard O, Hattori K, Hurn PD, Traystman RJ, Alkayed NJ. Social stress exacerbates stroke outcome by suppressing Bcl-2 expression. Proc Natl Acad Sci U S A. 2001;98(20):11824–8.

10. Sugo N, Hurn PD, Morahan MB, Hattori K, Traystman RJ, DeVries AC. Social stress exacerbates focal cerebral ischemia in mice. Stroke. 2002;33(6):1660–4.

11. Balkaya M, Prinz V, Custodis F, Gertz K, Kronenberg G, Kroeber J, Fink K, Plehm R, Gass P, Laufs U, Endres M. Stress worsens endothelial function and ischemic stroke via glucocorticoids. Stroke. 2011;42(11):3258–64.

12. Custodis F, Gertz K, Balkaya M, Prinz V, Mathar I, Stamm C, Kronenberg G, Kazakov A, Freichel M, Böhm M, Endres M, Laufs U. Heart rate contributes to the vascular effects of chronic mental stress: effects on endothelial function and ischemic brain injury in mice. Stroke. 2011;42(6):1742–9.

13. Endres M, Engelhardt B, Koistinaho J, Lindvall O, Meairs S, Mohr JP, Planas A, Rothwell N, Schwaninger M, Schwab ME, Vivien D, Wieloch T, Dirnagl U. Improving

outcome after stroke: overcoming the translational roadblock. Cerebrovasc Dis. 2008;25(3):268–78.

14. Raber J, Fan Y, Matsumori Y, Liu Z, Weinstein PR, Fike JR, Liu J. Irradiation attenuates neurogenesis and exacerbates ischemia-induced deficits. Ann Neurol. 2004;55(3):381–9.

15. Jin K, Wang X, Xie L, Mao XO, Greenberg DA. Transgenic ablation of doublecortin-expressing cells suppresses adult neurogenesis and worsens stroke outcome in mice. Proc Natl Acad Sci U S A. 2010;107(17):7993–8.

16. Gertz K, Priller J, Kronenberg G, Fink KB, Winter B, Schröck H, Ji S, Milosevic M, Harms C, Böhm M, Dirnagl U, Laufs U, Endres M. Physical activity improves long-term stroke outcome via endothelial nitric oxide synthase-dependent augmentation of neovascularization and cerebral blood flow. Circ Res. 2006;99(10):1132–40.

17. Gertz K, Kronenberg G, Kälin RE, Baldinger T, Werner C, Balkaya M, Eom GD, Hellmann-Regen J, Kröber J, Miller KR, Lindauer U, Laufs U, Dirnagl U, Heppner FL, Endres M. Essential role of interleukin-6 in post-stroke angiogenesis. Brain. 2012;135(6):1964–80.

18. Hoffmann CJ, Harms U, Rex A, Szulzewsky F, Wolf SA, Grittner U, Lättig-Tünnemann G, Sendtner M, Kettenmann H, Dirnagl U, Endres M, Harms C. Vascular signal transducer and activator of transcription-3 promotes angiogenesis and neuroplasticity long-term after stroke. Circulation. 2015;131(20):1772–82.

19. Ohab JJ, Fleming S, Blesch A, Carmichael ST. A neurovascular niche for neurogenesis after stroke. J Neurosci. 2006;26(50):13007–16.

20. Yamashita T, Ninomiya M, Hernández-Acosta P, García-Verdugo JM, Sunabori T, Sakaguchi M, Adachi K, Kojima T, Hirota Y, Kawase T, Araki N, Abe K, Okano H, Sawamoto K. Subventricular zone-derived neuroblasts migrate and differentiate into mature neurons in the post-stroke adult striatum. J Neurosci. 2006;26(24):6627–36.

21. Ulrich-Lai YM, Herman JP. Neural regulation of endocrine and autonomic stress responses. Nat Rev Neurosci. 2009;10(6):397–409.

22. Herman JP, Ostrander MM, Mueller NK, Figueiredo H. Limbic system mechanisms of stress regulation: hypothalamo-pituitary-adrenocortical axis. Prog Neuropsychopharmacol Biol Psychiatry. 2005;29(8):1201–13.

23. Hyman SE. How adversity gets under the skin. Nat Neurosci. 2009;12(3):241–3.

24. Lightman SL. The neuroendocrinology of stress: a never ending story. J Neuroendocrinol. 2008;20(6):880–4.

25. de Quervain D, Schwabe L, Roozendaal B. Stress, glucocorticoids and memory: implications for treating fear-related disorders. Nat Rev Neurosci. 2017;18(1):7–19.

26. Diorio D, Viau V, Meaney MJ. The role of the medial prefrontal cortex (cingulate gyrus) in the regulation of hypothalamic-pituitary-adrenal responses to stress. J Neurosci. 1993;13(9):3839–47.

27. Di S, Malcher-Lopes R, Halmos KC, Tasker JG. Nongenomic glucocorticoid inhibition via endocannabinoid release in the hypothalamus: a fast feedback mechanism. J Neurosci. 2003;23(12):4850–7.

28. Groeneweg FL, Karst H, de Kloet ER, Joëls M. Rapid non-genomic effects of corticosteroids and their role in the central stress response. J Endocrinol. 2011;209(2):153–67.

29. Russell G, Lightman S. The human stress response. Nat Rev Endocrinol. 2019;15(9):525–34.

30. Liu W, Wang J, Sauter NK, Pearce D. Steroid receptor heterodimerization demonstrated in vitro and in vivo. Proc Natl Acad Sci U S A. 1995;92(26):12480–4.

31. Karin M. New twists in gene regulation by glucocorticoid receptor: is DNA binding dispensable? Cell. 1998;93(4):487–90.

32. Grossmann C, Ruhs S, Langenbruch L, Mildenberger S, Strätz N, Schumann K, Gekle M. Nuclear shuttling precedes dimerization in mineralocorticoid receptor signaling. Chem Biol. 2012;19(6):742–51.

33. Whitfield GK, Jurutka PW, Haussler CA, Haussler MR. Steroid hormone receptors: evolution, ligands, and molecular basis of biologic function. J Cell Biochem. 1999;Suppl 32-3:110–22.

34. Groeneweg FL, Karst H, de Kloet ER, Joëls M. Mineralocorticoid and glucocorticoid receptors at the neuronal membrane, regulators of nongenomic corticosteroid signalling. Mol Cell Endocrinol. 2012;350(2):299–309.

35. Morimoto M, Morita N, Ozawa H, Yokoyama K, Kawata M. Distribution of glucocorticoid receptor immunoreactivity and mRNA in the rat brain: an immunohistochemical and in situ hybridization study. Neurosci Res. 1996;26(3):235–69.

36. Ahima R, Krozowski Z, Harlan R. Type I corticosteroid receptor-like immunoreactivity in the rat CNS: distribution and regulation by corticosteroids. J Comp Neurol. 1991;313(3):522–38.

37. Reul JMHM, de Kloet ER. Two receptor systems for corticosterone in rat brain: microdistribution and differential occupation. Endocrinology. 1985;117(6):2505–11.

38. Arriza JL, Weinberger C, Cerelli G, Glaser TM, Handelin BL, Housman DE, Evans RM. Cloning of human mineralocorticoid receptor complementary DNA: structural and functional kinship with the glucocorticoid receptor. Science. 1987;237(4812):268–75.

39. Sheppard KE, Funder JW. Equivalent affinity of aldosterone and corticosterone for type I receptors in kidney and hippocampus: direct binding studies. J Steroid Biochem. 1987;28(6):737–42.

40. Geerling JC, Loewy AD. Aldosterone in the brain. Am J Physiol Ren Physiol. 2009;297(3):F559-76.

41. Bradbury MJ, Akana SF, Dallman MF. Roles of type I and II corticosteroid receptors in regulation of basal activity in the hypothalamo-pituitary-adrenal axis during the diurnal trough and the peak: evidence for a nonadditive effect of combined receptor occupation. Endocrinology. 1994;134(3):1286–96.

42. Ratka A, Sutanto W, Bloemers M, de Kloet ER. On the role of brain mineralocorticoid (type I) and glucocorticoid (type II) receptors in neuroendocrine regulation. Neuroendocrinology. 1989;50(2):117–23.

43. Pariante CM, Miller AH. Glucocorticoid receptors in major depression: relevance to pathophysiology and treatment. Biol Psychiatry. 2001;49(5):391–404.

44. Renoir JM, Radanyi C, Faber LE, Baulieu EE. The non-DNA-binding heterooligomeric form of mammalian steroid hormone receptors contains a hsp90-bound 59-kilodalton protein. J Biol Chem. 1990;265(18):10740–5.

45. Barent RL, Nair SC, Carr DC, Ruan Y, Rimerman RA, Fulton J, Zhang Y, Smith DF. Analysis of FKBP51/FKBP52 chimeras and mutants for hsp90 binding and association

with progesterone receptor complexes. Mol Endocrinol. 1998;12(3):342–54.

46. Gallo LI, Ghini AA, Piwien-Pilipuk G, Galigniana MD. Differential recruitment of tetratricorpeptide repeat domain immunophilins to the mineralocorticoid receptor influences both heat-shock protein 90-dependent retrotransport and hormone-dependent transcriptional activity. Biochemistry. 2007;46(49):14044–57.

47. Wochnik GM, Rüegg J, Abel GA, Schmidt U, Holsboer F, Rein T. FK506-binding proteins 51 and 52 differentially regulate dynein interaction and nuclear translocation of the glucocorticoid receptor in mammalian cells. J Biol Chem. 2005;280(6):4609–16.

48. Febbo PG, Lowenberg M, Thorner AR, Brown M, Loda M, Golub TR. Androgen mediated regulation and functional implications of FKBP51 expression in prostate cancer. J Urol. 2005;173(5):1772–7.

49. Shrestha S, Sun Y, Lufkin T, Kraus P, Or Y, Garcia YA, Guy N, Ramos P, Cox MB, Tay F, Lin VCL. Tetratricopeptide repeat domain 9A negatively regulates estrogen receptor alpha activity. Int J Biol Sci. 2015;11(4):434–47.

50. Davies TH, Ning YM, Sánchez ER. A new first step in activation of steroid receptors: hormone-induced switching of FKBP51 and FKBP52 immunophilins. J Biol Chem. 2002;277(7):4597–600.

51. Galigniana MD, Radanyi C, Renoir JM, Housley PR, Pratt WB. Evidence that the peptidylprolyl isomerase domain of the hsp90-binding immunophilin FKBP52 is involved in both dynein interaction and glucocorticoid receptor movement to the nucleus. J Biol Chem. 2001;276(18):14884–9.

52. Galigniana MD, Harrell JM, Murphy PJM, Chinkers M, Radanyi C, Renoir JM, Zhang M, Pratt WB. Binding of hsp90-associated immunophilins to cytoplasmic dynein: direct binding and in vivo evidence that the peptidylprolyl isomerase domain is a dynein interaction domain. Biochemistry. 2002;41(46):13602–10.

53. Denny WB, Valentine DL, Reynolds PD, Smith DF, Scammell JG. Squirrel monkey immunophilin FKBP51 is a potent inhibitor of glucocorticoid receptor binding. Endocrinology. 2000;141(11):4107–13.

54. Reynolds PD, Ruan Y, Smith DF, Scammell JG. Glucocorticoid resistance in the squirrel monkey is associated with overexpression of the immunophilin FKBP51. J Clin Endocrinol Metab. 1999;84(2):663–9.

55. Vermeer H, Hendriks-Stegeman BI, van der Burg B, van Buul-Offers SC, Jansen M. Glucocorticoid-induced increase in lymphocytic FKBP51 messenger ribonucleic acid expression: a potential marker for glucocorticoid sensitivity, potency, and bioavailability. J Clin Endocrinol Metab. 2003;88(1):277–84.

56. Paakinaho V, Makkonen H, Jääskeläinen T, Palvimo JJ. Glucocorticoid receptor activates poised FKBP51 locus through long-distance interactions. Mol Endocrinol. 2010;24(3):511–25.

57. Scammell JG, Denny WB, Valentine DL, Smith DF. Overexpression of the FK506-binding immunophilin FKBP51 is the common cause of glucocorticoid resistance in three New World primates. Gen Comp Endocrinol. 2001;124(2):152–65.

58. Westberry JM, Sadosky PW, Hubler TR, Gross KL, Scammell JG. Glucocorticoid resistance in squirrel monkeys results from a combination of a transcriptionally incompetent glucocorticoid receptor and overexpression of the glucocorticoid receptor co-chaperone FKBP51. J Steroid Biochem Mol Biol. 2006;100(1–3):34–41.

59. Scharf SH, Liebl C, Binder EB, Schmidt MV, Müller MB. Expression and regulation of

the Fkbp5 gene in the adult mouse brain. PLoS One. 2011;6(2):e16883.

60. Blair LJ, Nordhues BA, Hill SE, Scaglione KM, O'Leary 3rd JC, Fontaine SN, Breydo L, Zhang B, Li P, Wang L, Cotman C, Paulson HL, Muschol M, Uversky VN, Klengel T, Binder EB, Kayed R, Golde TE, Berchtold N, Dickey CA. Accelerated neurodegeneration through chaperone-mediated oligomerization of tau. J Clin Invest. 2013;123(10):4158–69.

61. Zannas AS, Jia M, Hafner K, Baumert J, Wiechmann T, Pape JC, Arloth J, Ködel M, Martinelli S, Roitman M, Röh S, Haehle A, Emeny RT, Iurato S, Carrillo-Roa T, Lahti J, Räikkönen K, Eriksson JG, Drake AJ, Waldenberger M, Wahl S, Kunze S, Lucae S, Bradley B, Gieger C, Hausch F, Smith AK, Ressler KJ, Müller-Myhsok B, Ladwig KH, Rein T, Gassen NC, Binder EB. Epigenetic upregulation of FKBP5 by aging and stress contributes to NF-κB-driven inflammation and cardiovascular risk. Proc Natl Acad Sci U S A. 2019;116(23):11370–9.

62. Ising M, Depping AM, Siebertz A, Lucae S, Unschuld PG, Kloiber S, Horstmann S, Uhr M, Müller-Myhsok B, Holsboer F. Polymorphisms in the FKBP5 gene region modulate recovery from psychosocial stress in healthy controls. Eur J Neurosci. 2008;28(2):389–98.

63. Yekta S, Shih IH, Bartel DP. MicroRNA-directed cleavage of HOXB8 mRNA. Science. 2004;304(5670):594–6.

64. Zeng Y, Yi R, Cullen BR. MicroRNAs and small interfering RNAs can inhibit mRNA expression by similar mechanisms. Proc Natl Acad Sci U S A. 2003;100(17):9779–84.

65. Olsen PH, Ambros V. The lin-4 regulatory RNA controls developmental timing in Caenorhabditis elegans by blocking LIN-14 protein synthesis after the initiation of translation. Dev Biol. 1999;216(2):671–80.

66. Ketting RF, Fischer SEJ, Bernstein E, Sijen T, Hannon GJ, Plasterk RHA. Dicer functions in RNA interference and in synthesis of small RNA involved in developmental timing in C. elegans. Genes Dev. 2001;15(20):2654–9.

67. Lee Y, Ahn C, Han J, Choi H, Kim J, Yim J, Lee J, Provost P, Rådmark O, Kim S, Kim VN. The nuclear RNase III Drosha initiates microRNA processing. Nature. 2003;425(6956):415–9.

68. Lee Y, Jeon K, Lee JT, Kim S, Kim VN. MicroRNA maturation: stepwise processing and subcellular localization. EMBO J. 2002;21(17):4663–70.

69. Yi R, Qin Y, Macara IG, Cullen BR. Exportin-5 mediates the nuclear export of pre-microRNAs and short hairpin RNAs. Genes Dev. 2003;17(24):3011–6.

70. Lund E, Güttinger S, Calado A, Dahlberg JE, Kutay U. Nuclear export of microRNA precursors. Science. 2004;303(5654):95–8.

71. Hammond SM, Bernstein E, Beach D, Hannon GJ. An RNA-directed nuclease mediates post-transcriptional gene silencing in Drosophila cells. Nature. 2000;404(6775):293–6.

72. MacRae IJ, Ma E, Zhou M, Robinson CV, Doudna JA. In vitro reconstitution of the human RISC-loading complex. Proc Natl Acad Sci U S A. 2008;105(2):512–7.

73. Schwarz DS, Hutvágner G, Haley B, Zamore PD. Evidence that siRNAs function as guides, not primers, in the Drosophila and human RNAi pathways. Mol Cell. 2002;10(3):537–48.

74. Wu S, Huang S, Ding J, Zhao Y, Liang L, Liu T, Zhan R, He X. Multiple microRNAs modulate p21Cip1/Waf1 expression by directly targeting its 3' untranslated region.

Oncogene. 2010;29(15):2302–8.

75. Bommer GT, Gerin I, Feng Y, Kaczorowski AJ, Kuick R, Love RE, Zhai Y, Giordano TJ, Qin ZS, Moore BB, MacDougald OA, Cho KR, Fearon ER. p53-mediated activation of miRNA34 candidate tumor-suppressor genes. Curr Biol. 2007;17(15):1298–307.

76. Badi I, Burba I, Ruggeri C, Zeni F, Bertolotti M, Scopece A, Pompilio G, Raucci A. MicroRNA-34a induces vascular smooth muscle cells senescence by SIRT1 downregulation and promotes the expression of age-associated pro-inflammatory secretory factors. J Gerontol A Biol Sci Med Sci. 2015;70(11):1304–11.

77. Boon RA, Iekushi K, Lechner S, Seeger T, Fischer A, Heydt S, Kaluza D, Tréguer K, Carmona G, Bonauer A, Horrevoets AJG, Didier N, Girmatsion Z, Biliczki P, Ehrlich JR, Katus HA, Müller OJ, Potente M, Zeiher AM, Hermeking H, Dimmeler S. MicroRNA-34a regulates cardiac ageing and function. Nature. 2013;495(7439):107–10.

78. Ito T, Yagi S, Yamakuchi M. MicroRNA-34a regulation of endothelial senescence. Biochem Biophys Res Commun. 2010;398(4):735–40.

79. Li X, Khanna A, Li N, Wang E. Circulatory mir-34a as an RNA-based, noninvasive biomarker for brain aging. Aging (Albany NY). 2011;3(10):985–1002.

80. Xu Q, Seeger FH, Castillo J, Iekushi K, Boon RA, Farcas R, Manavski Y, Li YG, Assmus B, Zeiher AM, Dimmeler S. Micro-RNA-34a contributes to the impaired function of bone marrow-derived mononuclear cells from patients with cardiovascular disease. J Am Coll Cardiol. 2012;59(23):2107–17.

81. Yang Y, Cheng HW, Qiu Y, Dupee D, Noonan M, Lin YD, Fisch S, Unno K, Sereti KI, Liao R. MicroRNA-34a plays a key role in cardiac repair and regeneration following myocardial infarction. Circ Res. 2015;117(5):450–9.

82. Bukeirat M, Sarkar SN, Hu H, Quintana DD, Simpkins JW, Ren X. MiR-34a regulates blood-brain barrier permeability and mitochondrial function by targeting cytochrome c. J Cereb Blood Flow Metab. 2016;36(2):387–92.

83. Yamakuchi M, Ferlito M, Lowenstein CJ. miR-34a repression of SIRT1 regulates apoptosis. Proc Natl Acad Sci U S A. 2008;105(36):13421–6.

84. Brunet A, Sweeney LB, Sturgill JF, Chua KF, Greer PL, Lin Y, Tran H, Ross SE, Mostoslavsky R, Cohen HY, Hu LS, Cheng HL, Jedrychowski MP, Gygi SP, Sinclair DA, Alt FW, Greenberg ME. Stress-dependent regulation of FOXO transcription factors by the SIRT1 deacetylase. Science. 2004;303(5666):2011–5.

85. Vaziri H, Dessain SK, Ng Eaton E, Imai S, Frye RA, Pandita TK, Guarente L, Weinberg RA. hSIR2(SIRT1) functions as an NAD-dependent p53 deacetylase. Cell. 2001;107(2):149–59.

86. Dioum EM, Chen R, Alexander MS, Zhang Q, Hogg RT, Gerard RD, Garcia JA. Regulation of hypoxia-inducible factor 2α signaling by the stress-responsive deacetylase sirtuin 1. Science. 2009;324(5932):1289–93.

87. Luo J, Nikolaev AY, Imai S, Chen D, Su F, Shiloh A, Guarente L, Gu W. Negative control of p53 by Sir2α promotes cell survival under stress. Cell. 2001;107(2):137–48.

88. Potente M, Ghaeni L, Baldessari D, Mostoslavasky R, Rossig L, Dequiedt F, Haendeler J, Mione M, Dejana E, Alt FW, Zeiher AM, Dimmeler S. SIRT1 controls endothelial angiogenic functions during vascular growth. Genes Dev. 2007;21(20):2644–58.

89. Chang TC, Wentzel EA, Kent OA, Ramachandran K, Mullendore M, Lee KH, Feldmann G, Yamakuchi M, Ferlito M, Lowenstein CJ, Arking DE, Beer MA, Maitra A, Mendell JT.

Transactivation of miR-34a by p53 broadly influences gene expression and promotes apoptosis. Mol Cell. 2007;26(5):745–52.

90. Tazawa H, Tsuchiya N, Izumiya M, Nakagama H. Tumor-suppressive miR-34a induces senescence-like growth arrest through modulation of the E2F pathway in human colon cancer cells. Proc Natl Acad Sci U S A. 2007;104(39):15472–7.

91. Tarasov V, Jung P, Verdoodt B, Lodygin D, Epanchintsev A, Menssen A, Meister G, Hermeking H. Differential regulation of microRNAs by p53 revealed by massively parallel sequencing: miR-34a is a p53 target that induces apoptosis and G1-arrest. Cell Cycle. 2007;6(13):1586–93.

92. Misso G, Di Martino MT, De Rosa G, Farooqi AA, Lombardi A, Campani V, Zarone MR, Gullà A, Tagliaferri P, Tassone P, Caraglia M. Mir-34: a new weapon against cancer? Mol Ther Nucleic Acids. 2014;3(9):e194.

93. Gould E, Tanapat P, McEwen BS, Flügge G, Fuchs E. Proliferation of granule cell precursors in the dentate gyrus of adult monkeys is diminished by stress. Proc Natl Acad Sci U S A. 1998;95(6):3168–71.

94. Sapolsky RM, Krey LC, McEwen BS. Prolonged glucocorticoid exposure reduces hippocampal neuron number: implications for aging. J Neurosci. 1985;5(5):1222–7.

95. Vyas A, Mitra R, Shankaranarayana Rao BS, Chattarji S. Chronic stress induces contrasting patterns of dendritic remodeling in hippocampal and amygdaloid neurons. J Neurosci. 2002;22(15):6810–8.

96. Tynan RJ, Naicker S, Hinwood M, Nalivaiko E, Buller KM, Pow DV, Day TA, Walker FR. Chronic stress alters the density and morphology of microglia in a subset of stress-responsive brain regions. Brain Behav Immun. 2010;24(7):1058–68.

97. Sugama S, Fujita M, Hashimoto M, Conti B. Stress induced morphological microglial activation in the rodent brain: involvement of interleukin-18. Neuroscience. 2007;146(3):1388–99.

98. Gertz K, Kronenberg G, Uhlemann R, Prinz V, Marquina R, Corada M, Dejana E, Endres M. Partial loss of VE-cadherin improves long-term outcome and cerebral blood flow after transient brain ischemia in mice. BMC Neurol. 2016;16(1):144.

99. Strekalova T, Spanagel R, Bartsch D, Henn FA, Gass P. Stress-induced anhedonia in mice is associated with deficits in forced swimming and exploration. Neuropsychopharmacology. 2004;29(11):2007–17.

100. Dirnagl U, Members of the MCAO-SOP Group. Standard operating procedures (SOP) in experimental stroke research: SOP for middle cerebral artery occlusion in the mouse. Nat Preced. 2012.

101. Gerriets T, Stolz E, Walberer M, Müller C, Kluge A, Bachmann A, Fisher M, Kaps M, Bachmann G. Noninvasive quantification of brain edema and the space-occupying effect in rat stroke models using magnetic resonance imaging. Stroke. 2004;35(2):566–71.

102. Dobin A, Davis CA, Schlesinger F, Drenkow J, Zaleski C, Jha S, Batut P, Chaisson M, Gingeras TR. STAR: ultrafast universal RNA-seq aligner. Bioinformatics. 2013;29(1):15–21.

103. Anders S, Pyl PT, Huber W. HTSeq - a Python framework to work with high-throughput sequencing data. Bioinformatics. 2015;31(2):166–9.

104. Babicki S, Arndt D, Marcu A, Liang Y, Grant JR, Maciejewski A, Wishart DS.

Heatmapper: web-enabled heat mapping for all. Nucleic Acids Res. 2016;44(Web Server issue):W147–53.

105. Cahoy JD, Emery B, Kaushal A, Foo LC, Zamanian JL, Christopherson KS, Xing Y, Lubischer JL, Krieg PA, Krupenko SA, Thompson WJ, Barres BA. A transcriptome database for astrocytes, neurons, and oligodendrocytes: a new resource for understanding brain development and function. J Neurosci. 2008;28(1):264–78.

106. Wiedenmann B, Franke WW. Identification and localization of synaptophysin, an integral membrane glycoprotein of Mr 38,000 characteristic of presynaptic vesicles. Cell. 1985;41(3):1017–28.

107. Dinsmore JH, Solomon F. Inhibition of MAP2 expression affects both morphological and cell division phenotypes of neuronal differentiation. Cell. 1991;64(4):817–26.

108. Chawla A, Barak Y, Nagy L, Liao D, Tontonoz P, Evans RM. PPAR-γ dependent and independent effects on macrophage-gene expression in lipid metabolism and inflammation. Nat Med. 2001;7(1):48–52.

109. Ito D, Imai Y, Ohsawa K, Nakajima K, Fukuuchi Y, Kohsaka S. Microglia-specific localisation of a novel calcium binding protein, Iba1. Brain Res Mol Brain Res. 1998;57(1):1–9.

110. Zakrzewska A, Cui C, Stockhammer OW, Benard EL, Spaink HP, Meijer AH. Macrophage-specific gene functions in Spi1-directed innate immunity. Blood. 2010;116(3):e1–11.

111. Mustonen T, Alitalo K. Endothelial receptor tyrosine kinases involved in angiogenesis. J Cell Biol. 1995;129(4):895–8.

112. Stevenson BR, Siliciano JD, Mooseker MS, Goodenough DA. Identification of ZO-1: a high molecular weight polypeptide associated with tight junction (zonula occludens) in a variety of epithelia. J Cell Biol. 1986;103(3):755–66.

113. Heberle H, Meirelles GV, da Silva FR, Telles GP, Minghim R. InteractiVenn: a web-based tool for the analysis of sets through Venn diagrams. BMC Bioinformatics. 2015;16(1):169.

114. Reimand J, Arak T, Adler P, Kolberg L, Reisberg S, Peterson H, Vilo J. g:Profiler-a web server for functional interpretation of gene lists (2016 update). Nucleic Acids Res. 2016;44(Web Server issue):W83–9.

115. Supek F, Bošnjak M, Škunca N, Šmuc T. REVIGO summarizes and visualizes long lists of gene ontology terms. PLoS One. 2011;6(7):e21800.

116. Hammamieh R, Chakraborty N, De Lima TCM, Meyerhoff J, Gautam A, Muhie S, D'Arpa P, Lumley L, Carroll E, Jett M. Murine model of repeated exposures to conspecific trained aggressors simulates features of post-traumatic stress disorder. Behav Brain Res. 2012;235(1):55–66.

117. Patterson ZR, Khazall R, MacKay H, Anisman H, Abizaid A. Central ghrelin signaling mediates the metabolic response of C57BL/6 male mice to chronic social defeat stress. Endocrinology. 2013;154(3):1080–91.

118. Savignac HM, Finger BC, Pizzo RC, O'Leary OF, Dinan TG, Cryan JF. Increased sensitivity to the effects of chronic social defeat stress in an innately anxious mouse strain. Neuroscience. 2011;192:524–36.

119. Warren BL, Vialou VF, Iñiguez SD, Alcantara LF, Wright KN, Feng J, Kennedy PJ, LaPlant Q, Shen L, Nestler EJ, Bolaños-Guzmán CA. Neurobiological sequelae of

witnessing stressful events in adult mice. Biol Psychiatry. 2013;73(1):7–14.

120. Sutanto W, de Kloet ER. The use of various animal models in the study of stress and stress-related phenomena. Lab Anim. 1994;28(4):293–306.

121. Holsboer F, Spengler D, Heuser I. The role of corticotropin-releasing hormone in the pathogenesis of Cushing's disease, anorexia nervosa, alcoholism, affective disorders and dementia. Prog Brain Res. 1992;93:385–417.

122. Buwalda B, de Boer SF, Van Kalkeren AA, Koolhaas JM. Physiological and behavioral effects of chronic intracerebroventricular infusion of corticotropin-releasing factor in the rat. Psychoneuroendocrinology. 1997;22(5):297–309.

123. Wang SS, Kamphuis W, Huitinga I, Zhou JN, Swaab DF. Gene expression analysis in the human hypothalamus in depression by laser microdissection and real-time PCR: the presence of multiple receptor imbalances. Mol Psychiatry. 2008;13(8):786–99.

124. Raadsheer FC, van Heerikhuize JJ, Lucassen PJ, Hoogendijk WJG, Tilders FJH, Swaab DF. Corticotropin-releasing hormone mRNA levels in the paraventricular nucleus of patients with Alzheimer's disease and depression. Am J Psychiatry. 1995;152(9):1372–6.

125. Hartmann J, Wagner KV, Liebl C, Scharf SH, Wang XD, Wolf M, Hausch F, Rein T, Schmidt U, Touma C, Cheung-Flynn J, Cox MB, Smith DF, Holsboer F, Müller MB, Schmidt MV. The involvement of FK506-binding protein 51 (FKBP5) in the behavioral and neuroendocrine effects of chronic social defeat stress. Neuropharmacology. 2012;62(1):332–9.

126. Makino S, Smith MA, Gold PW. Increased expression of corticotropin-releasing hormone and vasopressin messenger ribonucleic acid (mRNA) in the hypothalamic paraventricular nucleus during repeated stress: association with reduction in glucocorticoid receptor mRNA levels. Endocrinology. 1995;136(8):3299–309.

127. Herman JP, Adams D, Prewitt C. Regulatory changes in neuroendocrine stress-integrative circuitry produced by a variable stress paradigm. Neuroendocrinology. 1995;61(2):180–90.

128. Papadopoulou A, Siamatras T, Delgado-Morales R, Amin ND, Shukla V, Zheng YL, Pant HC, Almeida OFX, Kino T. Acute and chronic stress differentially regulate cyclin-dependent kinase 5 in mouse brain: implications to glucocorticoid actions and major depression. Transl Psychiatry. 2015;5(6):e578.

129. Adzic M, Djordjevic J, Djordjevic A, Niciforovic A, Demonacos C, Radojcic M, Krstic-Demonacos M. Acute or chronic stress induce cell compartment-specific phosphorylation of glucocorticoid receptor and alter its transcriptional activity in Wistar rat brain. J Endocrinol. 2009;202(1):87–97.

130. Chen W, Dang T, Blind RD, Wang Z, Cavasotto CN, Hittelman AB, Rogatsky I, Logan SK, Garabedian MJ. Glucocorticoid receptor phosphorylation differentially affects target gene expression. Mol Endocrinol. 2008;22(8):1754–66.

131. Kino T, Ichijo T, Amin ND, Kesavapany S, Wang Y, Kim N, Rao S, Player A, Zheng YL, Garabedian MJ, Kawasaki E, Pant HC, Chrousos GP. Cyclin-dependent kinase 5 differentially regulates the transcriptional activity of the glucocorticoid receptor through phosphorylation: clinical implications for the nervous system response to glucocorticoids and stress. Mol Endocrinol. 2007;21(7):1552–68.

132. Elliott E, Ezra-Nevo G, Regev L, Neufeld-Cohen A, Chen A. Resilience to social stress coincides with functional DNA methylation of the Crf gene in adult mice. Nat Neurosci. 2010;13(11):1351–3.

133. Targonski PV, Bonetti PO, Pumper GM, Higano ST, Holmes Jr DR, Lerman A. Coronary endothelial dysfunction is associated with an increased risk of cerebrovascular events. Circulation. 2003;107(22):2805–9.

134. Schächinger V, Britten MB, Zeiher AM. Prognostic impact of coronary vasodilator dysfunction on adverse long-term outcome of coronary heart disease. Circulation. 2000;101(16):1899–906.

135. Halcox JPJ, Schenke WH, Zalos G, Mincemoyer R, Prasad A, Waclawiw MA, Nour KRA, Quyyumi AA. Prognostic value of coronary vascular endothelial dysfunction. Circulation. 2002;106(6):653–8.

136. Mausbach BT, Roepke SK, Ziegler MG, Milic M, von Känel R, Dimsdale JE, Mills PJ, Patterson TL, Allison MA, Ancoli-Israel S, Grant I. Association between chronic caregiving stress and impaired endothelial function in the elderly. J Am Coll Cardiol. 2010;55(23):2599–606.

137. Kershaw KN, Lane-Cordova AD, Carnethon MR, Tindle HA, Liu K. Chronic stress and endothelial dysfunction: The Multi-Ethnic Study of Atherosclerosis (MESA). Am J Hypertens. 2017;30(1):75–80.

138. Broadley AJM, Korszun A, Abdelaal E, Moskvina V, Jones CJH, Nash GB, Ray C, Deanfield J, Frenneaux MP. Inhibition of cortisol production with metyrapone prevents mental stress-induced endothelial dysfunction and baroreflex impairment. J Am Coll Cardiol. 2005;46(2):344–50.

139. Ghiadoni L, Donald AE, Cropley M, Mullen MJ, Oakley G, Taylor M, O'Connor G, Betteridge J, Klein N, Steptoe A, Deanfield JE. Mental stress induces transient endothelial dysfunction in humans. Circulation. 2000;102(20):2473–8.

140. Spieker LE, Hürlimann D, Ruschitzka F, Corti R, Enseleit F, Shaw S, Hayoz D, Deanfield JE, Lüscher TF, Noll G. Mental stress induces prolonged endothelial dysfunction via endothelin-A receptors. Circulation. 2002;105(24):2817–20.

141. Becker KJ, McCarron RM, Ruetzler C, Laban O, Sternberg E, Flanders KC, Hallenbeck JM. Immunologic tolerance to myelin basic protein decreases stroke size after transient focal cerebral ischemia. Proc Natl Acad Sci U S A. 1997;94(20):10873–8.

142. Griffiths-Jones S, Saini HK, van Dongen S, Enright AJ. miRBase: tools for microRNA genomics. Nucleic Acids Res. 2008;36(Database issue):D154-158.

143. Okamura K, Phillips MD, Tyler DM, Duan H, Chou YT, Lai EC. The regulatory activity of microRNA* species has substantial influence on microRNA and 3′ UTR evolution. Nat Struct Mol Biol. 2008;15(4):354–63.

144. Su W, Hopkins S, Nesser NK, Sopher B, Silvestroni A, Ammanuel S, Jayadev S, Möller T, Weinstein J, Garden GA. The p53 transcription factor modulates microglia behavior through microRNA-dependent regulation of c-Maf. J Immunol. 2014;192(1):358–66.

145. Agostini M, Tucci P, Steinert JR, Shalom-Feuerstein R, Rouleau M, Aberdam D, Forsythe ID, Young KW, Ventura A, Concepcion CP, Han YC, Candi E, Knight RA, Mak TW, Melino G. microRNA-34a regulates neurite outgrowth, spinal morphology, and function. Proc Natl Acad Sci U S A. 2011;108(52):21099–104.

146. McCubbrey AL, Nelson JD, Stolberg VR, Blakely PK, McCloskey L, Janssen WJ, Freeman CM, Curtis JL. miR-34a negatively regulates efferocytosis by tissue macrophages in part via SIRT1. J Immunol. 2016;196(3):1366–75.

147. Hsu CP, Zhai P, Yamamoto T, Maejima Y, Matsushima S, Hariharan N, Shao D, Takagi H, Oka S, Sadoshima J. Silent information regulator 1 protects the heart from

ischemia/reperfusion. Circulation. 2010;122(21):2170–82.

148. Hattori Y, Okamoto Y, Maki T, Yamamoto Y, Oishi N, Yamahara K, Nagatsuka K, Takahashi R, Kalaria RN, Fukuyama H, Kinoshita M, Ihara M. Silent information regulator 2 homolog 1 counters cerebral hypoperfusion injury by deacetylating endothelial nitric oxide synthase. Stroke. 2014;45(11):3403–11.

149. Ding M, Lei J, Han H, Li W, Qu Y, Fu E, Fu F, Wang X. SIRT1 protects against myocardial ischemia-reperfusion injury via activating eNOS in diabetic rats. Cardiovasc Diabetol. 2015;14:143.

150. Hong DS, Kang YK, Borad M, Sachdev J, Ejadi S, Lim HY, Brenner AJ, Park K, Lee JL, Kim TY, Shin S, Becerra CR, Falchook G, Stoudemire J, Martin D, Kelnar K, Peltier H, Bonato V, Bader AG, Smith S, Kim S, O'Neill V, Beg MS. Phase 1 study of MRX34, a liposomal miR-34a mimic, in patients with advanced solid tumours. Br J Cancer. 2020;122(11):1630–7.

## Statutory declaration

I, Stephanie Wegner, by personally signing this document in lieu of an oath, hereby affirm that I prepared the submitted dissertation on the topic “Effects of psychosocial stress on vascular function” independently and without the support of third parties, and that I used no other sources and aids other than those stated.

All parts which are based on the publications or presentations of other authors, either in letter or in spirit, are specified as such in accordance with the citing guidelines. The sections on methodology (in particular regarding practical work, laboratory regulations, statistical processing) and results (in particular regarding figures, charts and tables) are exclusively my responsibility.

Furthermore, I declare that I have correctly marked all of the data, the analyses, and the conclusions generated from data obtained in collaboration with other persons, and that I have correctly marked my own contribution and the contributions of other persons (cf. declaration of contribution). I have correctly marked all texts or parts of texts that were generated in collaboration with other persons.

My contributions to any publications to this dissertation correspond to those stated in the below joint declaration made together with the supervisor. All publications created within the scope of the dissertation comply with the guidelines of the ICMJE (International Committee of Medical Journal Editors; www.icmje.org) on authorship. In addition, I declare that I shall comply with the regulations of Charité – Universitätsmedizin Berlin on ensuring good scientific practice.

I declare that I have not yet submitted this dissertation in identical or similar form to another Faculty.

The significance of this statutory declaration and the consequences of a false statutory declaration under criminal law (Sections 156, 161 of the German Criminal Code) are known to me.”

Date Signature

## Declaration of contribution

Stephanie Wegner contributed the following to the below listed publication:

Publication: Wegner S, Uhlemann R, Boujon V, Ersoy B, Endres M, Kronenberg G*, Gertz K*. Endothelial Cell-Specific Transcriptome Reveals Signature of Chronic Stress Related to Worse Outcome After Mild Transient Brain Ischemia in Mice. Mol Neurobiol. 2020; 57(3): 1446-1458.

* Authors contributed equally

<u>Stephanie Wegner's contribution in detail:</u>

- Design of the study together with PD Dr. Karen Gertz and Prof. Dr. Golo Kronenberg.
- Performance of the *in vivo* experiments:
    - Conduction of stress procedure (approx. 90%).
    - Execution of MRI scans. However, MRI data analysis including lesion size calculation was performed together with Melanie Kroh.
    - Animal handling, weighing of animals and adrenal glands, extensive monitoring after MCAo, and sample collection were performed together with Melanie Kroh, Stefanie Balz, Renate Franke, and Dr. Ria Uhlemann.
- Total RNA isolation, cDNA synthesis, qPCR, and agarose gel electrophoresis were performed with Bettina Herrmann (but cDNA synthesis for RNA-seq was performed by LGC Genomics GmbH).
- Preparation of hypothalamic lysate and protein concentration determination for Western Blot analysis.
- Western Blot analysis was performed together with Bettina Herrmann.
- Statistical analysis of the data shown in Fig 1, Fig 2b and Fig 4.
- Design and establishment of the endothelial cell isolation strategy.
- Endothelial cell enrichment with MACS for RNA-seq experiment was performed with the help of Dr. Ria Uhlemann and Bettina Herrmann.

- FACS staining.
- Cell sorting was performed with assistance of the Flow Cytometry Core Facility at the German Rheumatism Research Center Berlin.
- Set the definition of DEGs (initially, LGC Genomics GmbH defined all genes with FDR-adjusted *p*-value < 0.05 as DEGs independent of fold change value).
- Construction of the heatmap, Volcano plots, Venn diagram, summarized tables of DEGs together with performance of GO term analysis.
- Deposition of RNA-seq data in the NCBI Gene Expression Omnibus (GEO).
- Preparation of all tables, graphs (except for principal component analysis plot in Fig 2), and figures.
- Writing publication together with Prof. Dr. Golo Kronenberg, PD Dr. Karen Gertz, and Dr. Ria Uhlemann.
    - Initial preparation of manuscript and in part implementation of adjustments according to the feedback of the co-authors.
    - During revision, initial preparation of the point-by-point response and in part preparation of the final manuscript.

Stephanie Wegner, M.Sc.

## Web of Science - Excerpt from the Journal Summary List 2017, category: NEUROSCIENCES

Journal Data Filtered By: **Selected JCR Year: 2017** Selected Editions: SCIE,SSCI Selected Categories: **“NEUROSCIENCES”** Selected Category Scheme: WoS

**Total: 261 journals**

| Rank | Full Journal Title | Total Cites | Journal Impact Factor | Eigenfactor Score |
|---|---|---|---|---|
| 1 | NATURE REVIEWS NEUROSCIENCE | 40,834 | 32.635 | 0.069940 |
| 2 | NATURE NEUROSCIENCE | 59,426 | 19.912 | 0.153710 |
| 3 | ACTA NEUROPATHOLOGICA | 18,783 | 15.872 | 0.041490 |
| 4 | TRENDS IN COGNITIVE SCIENCES | 25,391 | 15.557 | 0.040790 |
| 5 | BEHAVIORAL AND BRAIN SCIENCES | 8,900 | 15.071 | 0.010130 |
| 6 | Annual Review of Neuroscience | 13,320 | 14.675 | 0.016110 |
| 7 | NEURON | 89,410 | 14.318 | 0.216730 |
| 8 | PROGRESS IN NEUROBIOLOGY | 13,065 | 14.163 | 0.015550 |
| 9 | BIOLOGICAL PSYCHIATRY | 42,494 | 11.982 | 0.056910 |
| 10 | MOLECULAR PSYCHIATRY | 18,460 | 11.640 | 0.047200 |
| 11 | JOURNAL OF PINEAL RESEARCH | 9,079 | 11.613 | 0.008600 |
| 12 | TRENDS IN NEUROSCIENCES | 20,061 | 11.439 | 0.026860 |
| 13 | BRAIN | 52,061 | 10.840 | 0.075170 |
| 14 | SLEEP MEDICINE REVIEWS | 6,080 | 10.602 | 0.010720 |
| 15 | ANNALS OF NEUROLOGY | 37,251 | 10.244 | 0.053390 |
| 16 | Translational Stroke Research | 2,202 | 8.266 | 0.005260 |

| | | | | |
|---|---|---|---|---|
| 17 | NEUROSCIENCE AND BIOBEHAVIORAL REVIEWS | 24,279 | 8.037 | 0.048460 |
| 18 | NEUROSCIENTIST | 4,738 | 7.461 | 0.008730 |
| 19 | NEURAL NETWORKS | 10,086 | 7.197 | 0.015290 |
| 20 | FRONTIERS IN NEUROENDOCRINOLOGY | 3,924 | 6.875 | 0.006040 |
| 21 | NEUROPSYCHOPHARMACOLOGY | 24,537 | 6.544 | 0.042870 |
| 22 | CURRENT OPINION IN NEUROBIOLOGY | 14,190 | 6.541 | 0.034670 |
| 23 | Molecular Neurodegeneration | 3,489 | 6.426 | 0.009850 |
| 24 | CEREBRAL CORTEX | 29,570 | 6.308 | 0.058970 |
| 25 | BRAIN BEHAVIOR AND IMMUNITY | 12,583 | 6.306 | 0.026850 |
| 26 | BRAIN PATHOLOGY | 4,952 | 6.187 | 0.007750 |
| 27 | Brain Stimulation | 4,263 | 6.120 | 0.014510 |
| 28 | NEUROPATHOLOGY AND APPLIED NEUROBIOLOGY | 3,654 | 6.059 | 0.006350 |
| 29 | JOURNAL OF CEREBRAL BLOOD FLOW AND METABOLISM | 19,450 | 6.045 | 0.028280 |
| 30 | JOURNAL OF NEUROSCIENCE | 176,157 | 5.970 | 0.265950 |
| 31 | Molecular Autism | 1,679 | 5.872 | 0.006320 |
| 31 | Translational Neurodegeneration | 589 | 5.872 | 0.002280 |
| 33 | GLIA | 13,417 | 5.846 | 0.020530 |
| 34 | Neurotherapeutics | 3,973 | 5.719 | 0.008980 |
| 35 | PAIN | 36,132 | 5.559 | 0.038000 |
| 36 | NEUROIMAGE | 92,719 | 5.426 | 0.152610 |
| 37 | Acta Neuropathologica Communications | 2,326 | 5.414 | 0.011550 |
| 38 | Multiple Sclerosis Journal | 10,675 | 5.280 | 0.021890 |

| | | | | |
|---|---|---|---|---|
| 39 | NEUROBIOLOGY OF DISEASE | 16,259 | 5.227 | 0.031390 |
| 40 | Journal of Neuroinflammation | 9,761 | 5.193 | 0.024860 |
| 41 | JOURNAL OF PSYCHIATRY & NEUROSCIENCE | 2,989 | 5.182 | 0.004700 |
| 42 | Annual Review of Vision Science | 227 | 5.140 | 0.001660 |
| 43 | SLEEP | 20,547 | 5.135 | 0.025870 |
| 44 | MOLECULAR NEUROBIOLOGY | 10,183 | 5.076 | 0.023310 |
| 45 | NEUROENDOCRINOLOGY | 4,670 | 5.024 | 0.005340 |
| 46 | Alzheimers Research & Therapy | 2,192 | 5.015 | 0.008470 |
| 47 | JOURNAL OF NEUROTRAUMA | 14,508 | 5.002 | 0.021130 |
| 48 | HUMAN BRAIN MAPPING | 20,334 | 4.927 | 0.042810 |
| 49 | CORTEX | 9,506 | 4.907 | 0.023240 |
| 50 | NEUROPSYCHOLOGY REVIEW | 2,996 | 4.894 | 0.004070 |

In category “Neurosciences”, the journal “Molecular Neurobiology” is on rank 44 from total 261 journals.

Molecular Neurobiology (2020) 57:1446–1458
https://doi.org/10.1007/s12035-019-01822-3

# Endothelial Cell-Specific Transcriptome Reveals Signature of Chronic Stress Related to Worse Outcome After Mild Transient Brain Ischemia in Mice

Stephanie Wegner [1] · Ria Uhlemann [1] · Valérie Boujon [1] · Burcu Ersoy [1] · Matthias Endres [1,2,3] · Golo Kronenberg [1,4] · Karen Gertz [1,2]

Received: 27 May 2019 / Accepted: 23 October 2019 / Published online: 22 November 2019


## Abstract

Vascular mechanisms underlying the adverse effects that depression and stress-related mental disorders have on stroke outcome are only partially understood. Identifying the transcriptomic signature of chronic stress in endothelium harvested from the ischemic brain is an important step towards elucidating the biological processes involved. Here, we subjected male 129S6/SvEv mice to a 28-day model of chronic stress. The ischemic lesion was quantified after 30 min filamentous middle cerebral artery occlusion (MCAo) and 48 h reperfusion by T2-weighted MRI. RNA sequencing was used to profile transcriptomic changes in cerebrovascular endothelial cells (ECs) from the infarct. Mice subjected to the stress procedure displayed reduced weight gain, increased adrenal gland weight, and increased hypothalamic FKBP5 mRNA and protein expression. Chronic stress conferred increased lesion volume upon MCAo. Stress-exposed mice showed a higher number of differentially expressed genes between ECs isolated from the ipsilateral and contralateral hemisphere than control mice. The genes in question are enriched for roles in biological processes closely linked to endothelial proliferation and neoangiogenesis. MicroRNA-34a was associated with nine of the top 10 biological process Gene Ontology terms selectively enriched in ECs from stressed mice. Moreover, expression of mature miR-34a-5p and miR-34a-3p in ischemic brain tissue was positively related to infarct size and negatively related to sirtuin 1 (*Sirt1*) mRNA transcription. In conclusion, this study represents the first EC-specific transcriptomic analysis of chronic stress in brain ischemia. The stress signature uncovered relates to worse stroke outcome and is directly relevant to endothelial mechanisms in the pathogenesis of stroke.

**Keywords** Psychological stress · Depression · HPA axis · Stroke · Endothelium

## Introduction

Chronic psychosocial stress is increasingly recognized as a clinically meaningful cardio- and cerebrovascular risk factor [1–3]. Endothelial dysfunction may represent an important pathophysiological link whereby psychosocial stress confers increased vascular vulnerability [4, 5]. Even brief episodes of mental stress have been shown to elicit rapid and robust, albeit transient, effects on endothelial function [6, 7]. Studies in healthy human subjects indicate that, besides activation of the sympathetic nervous system, dysregulation of the hypothalamic-pituitary-adrenal axis contributes critically to stress-induced endothelial impairment [7–10].

Evidence from experimental animal research indicates that chronic stress increases infarct volume [11, 12]. By combining a mouse model of chronic stress over 4 weeks with a model of mild transient brain ischemia (i.e., 30 min middle cerebral artery occlusion [MCAo]), we previously identified that the

Golo Kronenberg and Karen Gertz contributed equally to this work

**Electronic supplementary material** The online version of this article (https://doi.org/10.1007/s12035-019-01822-3) contains supplementary material, which is available to authorized users.

✉ Karen Gertz
karen.gertz@charite.de

1 Klinik für Neurologie, Charité Campus Mitte, Charité—Universitätsmedizin Berlin, Charitéplatz 1, 10117 Berlin, Germany

2 DZHK (German Center for Cardiovascular Research), Partner site Berlin, 10115 Berlin, Germany

3 Deutsches Zentrum für Neurodegenerative Erkrankungen (DZNE), 10117 Berlin, Germany

4 University of Leicester and Leicestershire Partnership NHS Trust, Leicester, UK

adverse effects of stress on the ischemic brain involve the endothelium. Mechanistically, both glucocorticoid signaling and a stress-related increase in heart rate were found to cause endothelial dysfunction [13, 14].

Building on this evidence, the current study was undertaken to further characterize the neuroendocrine features of the four week stress model. After confirming that the stress procedure leads to increased lesion volume, we performed RNA sequencing to examine changes in gene expression due to prior stress exposure in ex vivo endothelia harvested from the middle cerebral artery (MCA) territory. We report a transcriptomic signature of chronic stress in MCAo-exposed endothelium and identify upregulation of miRNA-34a as a novel factor promoting ischemic brain injury.

## Materials and Methods

### Animals

All animal studies and experimental procedures were approved by the necessary official committees and conducted in compliance with the requirements set out in the European Communities Council Directive of November 24, 1986 (86/609/EEC) and the ARRIVE guidelines [15]. Male 129S6/SvEv mice raised under specific-pathogen-free (SPF) conditions were provided by the Forschungseinrichtungen für Experimentelle Medizin (FEM) of the Charité Universitätsmedizin Berlin. Young adult male mice (~ 9 ± 1 weeks old) weighing between 24 and 30 g were randomly used for experiments. Animals were maintained in a temperature (22 °C ± 2 °C) and humidity (55% ± 10%) controlled environment with a 12:12 h light-dark cycle and ad-libitum access to food and water.

### Stress Procedure

A schematic of the experimental setup and timeline is given in Fig. 1a. Briefly, the stress procedure was adapted from previously published protocols [13, 14, 16].

#### Exposure to Rat

At the beginning of the dark phase, a single mouse was situated in a small cage with the following dimensions: height 140 mm, width 167 mm, length 252 mm. This small cage was then placed inside a larger rat cage (height 200 mm, width 375 mm, length 585 mm). A rat was introduced into the rat cage for 15 h (6 p.m. to 9 a.m.). A single session of exposure to rat was also used as the means to induce acute stress.

#### Restraint Stress

Animals were placed inside the restraining syringe (internal diameter 30 mm) for 1 h during the dark phase (7 p.m. to 8 p.m.).

#### Tail Suspension Stress

Mice were suspended by the tail approximately 80 cm above the ground for 6 min/day. The procedure started at 7 p.m.

### Induction of Cerebral Ischemia

The standard operating procedure ‘Middle cerebral artery occlusion in the mouse’ published by Dirnagl and members of the MCAO-SOP group was followed (for a more detailed description of the procedure please refer to http://precedings.nature.com/documents/3492/version/3/files/npre20123492-3.pdf). Briefly, mice were anaesthetized for induction with 1.5% isoflurane and maintained in 1.0% isoflurane in 69% $N_2O$ and 30% $O_2$ using a vaporizer. Left MCAo was induced with an 8.0 nylon monofilament coated with a silicone resin/hardener mixture (Xantopren M Mucosa and Activator NF Optosil Xantopren, Heraeus Kulzer GmbH). The filament was introduced into the internal carotid artery up to the anterior cerebral artery. Thereby, the middle cerebral artery and anterior choroidal arteries were occluded. The filament was removed after 30 min to allow reperfusion.

### Magnetic Resonance Imaging

Successful MCAo was confirmed by magnetic resonance imaging (MRI) using a 7 Tesla rodent scanner (PharmaScan® 70/16, Bruker Corp.) and a 20-mm $^1$H-RF quadrature-volume resonator. A T2-weighted 2D turbo spin-echo sequence was used (imaging parameters TR/TE = 4200/36 ms, rare factor 8, 4 averages, 32 axial slices with a slice thickness of 0.5 mm, field of view of 2.56 × 2.56 cm, matrix size 256 × 256). Throughout the procedure, animals were anaesthetized with 1–2% isoflurane in 70% $N_2O$ and 30% $O_2$. The respiratory rate was monitored with an MRI compatible small animal monitoring and gating system (SA Instruments, Inc.). Lesion volume was evaluated with Analyze 10.0 (AnalyzeDirect, Inc.) and corrected for edema according to a previously published protocol [17].

### Measurement of Adrenal Gland Weights and Corticosterone Plasma Levels

Corticosterone levels in plasma were determined by ELISA according to the manufacturer’s instructions (RE52211, IBL International GmbH). After sacrifice, the adrenal glands were dissected and weighed.

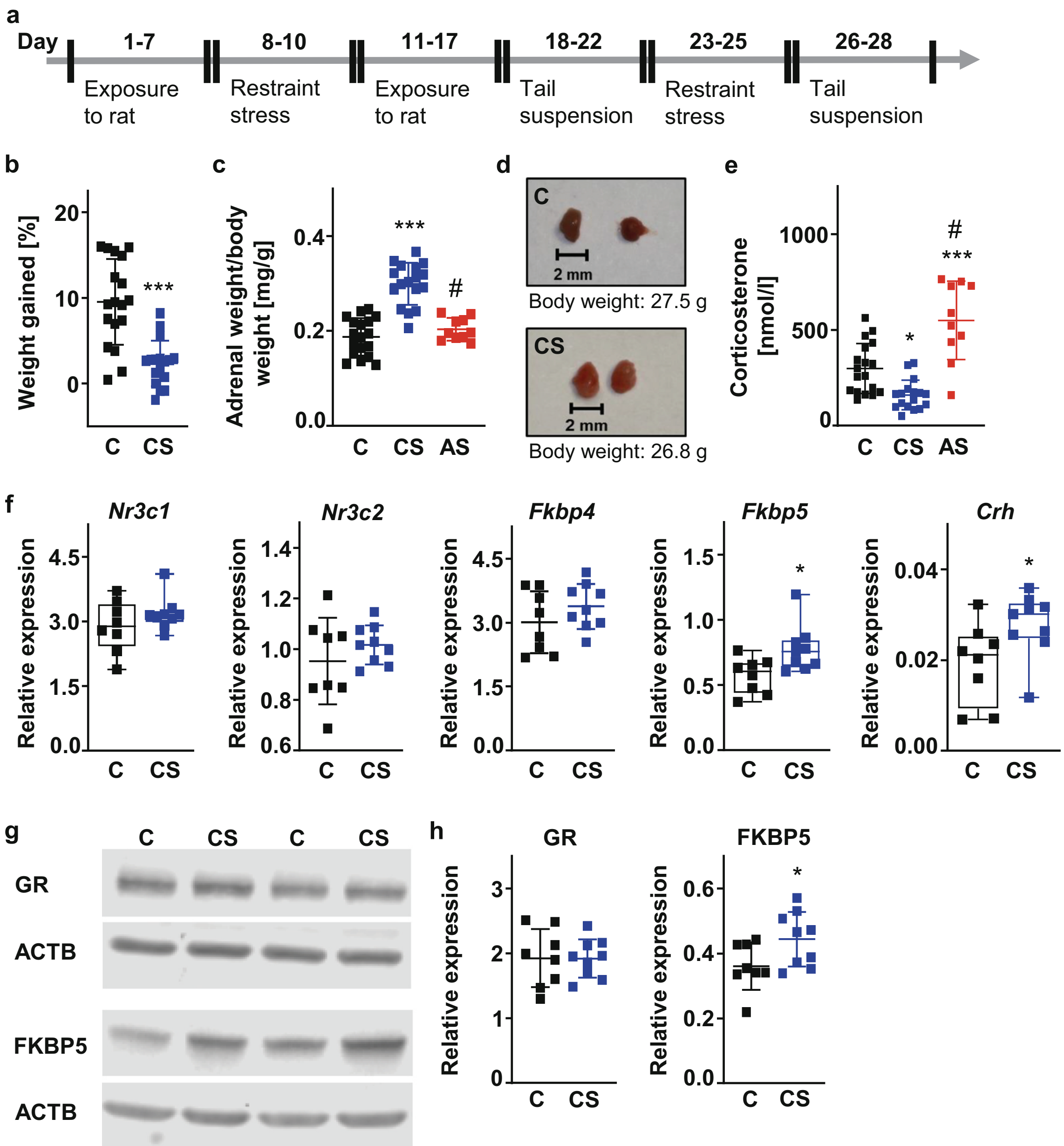


**Fig. 1** Characterization of the neuroendocrine effects of the chronic stress paradigm. **a** Schematic diagram of experimental design. **b** Body weight was recorded before the beginning and at the end of the chronic stress procedure. Chronically stressed mice gain less body weight than unstressed control animals. C: $n$ = 18, CS: $n$ = 17. Unpaired $t$ test. $t$ = 5.262, ***$p$ < 0.001. **c**, **d** Chronic stress increases the weight of the adrenal glands. C: $n$ = 18, CS: $n$ = 17, AS: $n$ = 10. One-way ANOVA F(2,42) = 40.14, $p$ < 0.001 with Tukey's multiple comparison test: ***$p$ < 0.001 CS versus C, #$p$ < 0.001 CS versus AS. **e** Corticosterone plasma levels were measured at the beginning of the light cycle. C: $n$ = 18, CS: $n$ = 17, AS: $n$ = 10. One-way ANOVA F(2,42) = 26.20, $p$ < 0.001 with Tukey's multiple comparison test: *$p$ < 0.05 CS versus C, ***$p$ < 0.001 AS versus C, #$p$ < 0.001 CS versus AS. **f** Hypothalamic mRNA transcription of genes associated with corticosteroid signaling. *Nr3c1*, nuclear receptor subfamily 3 group C member 1. *Nr3c2*, nuclear receptor subfamily 3 group C member 2. *Fkbp4*, FK506 binding protein 4. *Fkbp5*, FK506 binding protein 5. *Crh*, corticotropin releasing hormone. Relative mRNA expression is reported as the value normalized to tripeptidyl peptidase 2 (*Tpp2*) for each sample. C: $n$ = 8, CS: $n$ = 9. Mann-Whitney $U$ test. *Nr3c1*: $U$ = 27, $p$ = 0.423. *Fkbp5:* $U$ = 12, *$p$ < 0.05. *Crh:* $U$ = 14, *$p$ < 0.05. Unpaired $t$ test. *Nr3c2*: $t$ = 1.016, $p$ = 0.326. *Fkbp4*: $t$ = 1.214, $p$ = 0.244. **g** Representative Western blots of GR and FKBP5 protein expression in hypothalamic homogenates. GR, glucocorticoid receptor. FKBP5, FK506 binding protein 51. ACTB, β-actin. **h** Densitometric analysis. Values were normalized to β-actin. C: $n$ = 8, CS: $n$ = 9. Unpaired $t$ test. GR: $t$ = 0.029, $p$ = 0.977. FKBP5: $t$ = 2.173, *$p$ < 0.05. C, unstressed control mice. CS, chronically stressed mice. AS, acutely stressed mice

## RNA Isolation

Total RNA was extracted from hypothalamus and from ex vivo endothelial cells (ECs) using the NucleoSpin® XS Kit according to the manufacturer's protocol (MACHEREY-NAGEL GmbH & Co. KG). RNA isolation from ECs was performed without the addition of carrier RNA.

### Quantitative Polymerase Chain Reactions

Synthesis of cDNA was performed with 300 U M-MLV reverse transcriptase (Promega Corp.), 20 U RNasin® ribonuclease inhibitor (Promega Corp.), 4.76 mM DTT (Promega Corp.), 1.43 mM PCR nucleotide mix (Promega Corp.), and 6.28 μM random primers (Roche Diagnostics GmbH). For PCR amplification, we used gene-specific primers (Table 1) and LightCycler® 480 SYBR Green I Master (Roche Diagnostics GmbH). Polymerase chain reaction conditions were as follows: preincubation 95 °C, 10 min; 95 °C, 10 s, primer-specific annealing temperature, 10 s, 72 °C, 15 s (45 cycles). Crossing points of amplified products were determined using the Second Derivative Maximum Method (LightCycler® 480 Version 1.5.0 SP4, Roche). Quantification of messenger RNA expression was relative to tripeptidyl peptidase (Tpp) 2 [18]. The specificity of polymerase chain reaction products was evaluated by melting curve analysis and electrophoresis on a 1.5% agarose gel.

### MiRNA Isolation and Quantification

Total RNA (including the microRNA fraction) was isolated from ischemic brain tissue using the Direct-zol™ RNA MiniPrep Kit (Zymo Research Corp.). Tissue was homogenized with TRIzol™ Reagent (Invitrogen™) and TissueLyser LT (Qiagen) for 3 × 5 min at 50 Hz. Transcription of 500 ng total RNA into cDNA and real-time PCR was carried out with the miScript PCR Starter Kit (Qiagen). Custom miScript Primer Assays were used to detect miR-34a-5p, miR-34a-3p, and RNU6B (Qiagen). The level of miRNA expression in ischemic brain tissue of control mice and of chronically stressed mice was normalized to RNU6B (RNU6-2) using the $2^{(-\Delta\Delta Ct)}$ method [19]. Melting curve analysis and agarose gel electrophoresis confirmed specificity of polymerase chain reaction products.

### Western Blot

After sacrifice, brains were quickly removed, flash frozen in dry ice-cooled isopentane, and stored until further use. The hypothalamus was dissected on a cold plate (− 20 °C) according to Franklin and Paxinos (1997). Protein concentration was determined with the Pierce™ BCA Protein Assay Kit (ThermoFisher Scientific Inc.). Equal amounts of protein were loaded on 10% SDS-polyacrylamide gels and blotted onto Immobilon®-FL PVDF membranes (Merck KGaA). Near-infrared fluorescent signals were detected with the Odyssey® CLx Infrared Imaging System (LI-COR, Inc.). Densitometric quantification of band intensity was performed with the Image Studio™ Lite Software (LI-COR, Inc.). The following primary antibodies were used: rabbit anti-glucocorticoid receptor (#12041, Cell Signaling Technology, Inc.) 1:1000; rabbit anti-FKBP5 (#711292, ThermoFisher Scientific Inc.) 1:1000; mouse anti-beta actin (#ab8226, Abcam plc.) 1:2000. Secondary antibodies were used as follows: donkey anti-rabbit 800 (#925-32213, LI-COR, Inc.) 1:15000; donkey anti-mouse 680 (#925-32213, LI-COR, Inc.) 1:15000.

### Ex vivo Isolation of Brain ECs

Control (C) and chronically stressed mice (CS) were perfused transcardially with 0.9% saline. Brains were quickly removed. The ipsilateral ischemic MCA territory, as well as the corresponding area in the contralateral hemisphere, was carefully dissected and placed in cold PBS (4 °C). Brain tissue of 3–5 animals was pooled. CD31+ cells were enriched from brain tissue using a MACS protocol combined with prior myelin removal (Miltenyi Biotec GmbH). To ensure a high purity of ECs, an additional FACS step was performed. Cells were stained with DAPI and antibodies against CD31, CD146, and CD45. Single cells that were CD45-/DAPI-/CD31+/CD146+ were separated from the remainder of the suspension using a BD FACSAria™ II flow cytometer. For FACS staining, the following antibodies were used: anti-mouse CD31-Alexa Fluor® 488 (#102514, BioLegend, Inc.); anti-mouse CD45-APC (#130-102-544, Miltenyi Biotec GmbH); anti-mouse CD146 (LSEC)-PE (#130-102-319, Miltenyi Biotec GmbH).

### RNA Sequencing of Ex vivo ECs

Assessment of RNA quality, cDNA synthesis, library preparation, sequencing, data pre-processing, alignment, and principal component analysis (PCA) was conducted by LGC Genomics GmbH (Berlin, Germany). Libraries were prepared with the Encore Rapid DR Multiplex system (NuGEN Technologies, Inc.) according to the manufacturer's directions and sequenced with 150 bp paired-end reads on the Illumina® NextSeq™ 500. Data pre-processing involved the following steps: demultiplexing of all libraries with the Illumina® bcl2fastq 2.17.1.14 software, clipping of sequencing adapter remnants from all raw reads, merging of forward and reverse reads using BBMerge 34.48, SMRT concatamer adapter detection and read splitting, filtering of poly-A reads, and filtering of rRNA sequences with riboPicker 0.4.3 [20]. RNA-seq data have been deposited at the Gene Expression Omnibus (GEO) [21] under GEO accession number GSE122345.

### Analysis of Differentially Expressed Genes

A total of 400 million reads were aligned to the reference genome (*Mus musculus*; GRCm38; Ensembl version 84) using STAR 2.4.1b [22]. Reads mapping to rRNA or tRNA regions were filtered post-alignment. Counting of STAR-

**Table 1** Oligonucleotide sequences used in quantitative real-time polymerase chain reactions

| Gene | Sense | Antisense |
|---|---|---|
| *Crh* | CTA CCA AGG GAG GAG AAG AGA G | CTG CTC CGG CTG CAA GAA ATT C |
| *Fkbp4* | CGT GCT CAA GGT CAT CAA GAG AG | GTT GCC ACA GCA ATA TCC CAA GC |
| *Fkbp5* | GCA GGG TGA AGA TAT CAC TAC G | CCA ATG TCC CAG GCT TTG ATA AC |
| *Nr3c1* | GAC GTG TGG AAG CTG TAA AGT C | CCA GGT TCA TTC CAG CTT GAA G |
| *Nr3c2* | CAC ACG GTG ACC TGT CAT CTA G | CAT AGT GAC ACC CAG AAG CCT C |
| *Tpp2* | CTT CTA TCC AAA GGC TCT CAA GG | CTC TCC AGG TCT CAC CAT CAT G |
| *Sirt1* | CCA GAC CCT CAA GCC ATG TTT G | CTG CAA CCT GCT CCA AGG TAT C |

aligned reads was conducted using htseq-count [23]. FPKM values (fragments per kilobase per million fragments mapped) and differentially expressed genes (DEGs) analyses were calculated with Cuffdiff 2.1.1 by LGC Genomics GmbH (Berlin, Germany). The raw $p$ values from the statistical tests were adjusted for multiple testing by the Benjamini-Hochberg false discovery rate (FDR) method. Genes with an FDR-adjusted $p$ value < 0.05 and fold change ≥ 2 or ≤ − 2 were considered to be DEGs. When a gene cannot be detected in samples derived from one side of the brain, the log2(fold change) yields a value of infinity. In those instances in which the log2(fold change) yielded infinity and the FDR-adjusted $p$ value was < 0.05, the gene in question was still not regarded as differentially expressed because these genes also showed a very low mean count of < 4 on the other side of the brain (5 genes in the control mice [*Gm13755, Gm3191, Igkv4-58, Gm6064, 1700017I07Rik*]; 2 genes in the chronically stressed animals [*Gm24447, Gm11686*]). The Venn diagram (Fig. 3c) was created with a web-based tool [24]. The expression levels of different marker genes were visualized with heatmapper [25]. Specific markers for each cell population were collated from different publications [26–33].

## Gene Ontology Analysis

Gene ontology (GO) enrichment analysis was performed with g:Profiler [34; Ensembl version 91]. The size of functional categories was limited to between 5 and 5000 genes so as to reduce redundancy in GO annotation. The Benjamini-Hochberg false discovery rate (FDR) correction was calculated to adjust for multiple testing. GO annotations with an adjusted $p$ value < 0.01 were considered to be significantly enriched. Finally, REVIGO was used to filter out redundant categories [35].

## Statistics

Except for the stress experiments, all procedures and analyses were performed in a blinded fashion. Results are presented as individual values and as mean ± SD or as boxplot with median and interquartile range as appropriate. Mice were excluded from this study either when MRI yielded evidence of intracerebral hemorrhage (C: 0%, CS: 3%) or failed to confirm successful MCAo (C: 19%, CS: 21%). Statistical analysis was performed using GraphPad Prism version 7 or 8 (GraphPad Software, Inc.). Normality testing was done using D'Agostino-Pearson omnibus test ($n \geq 8$) or Shapiro-Wilk test ($n < 8$). Since the present study was designed as an exploratory investigation, we did not correct for multiple comparisons.

# Results

## Neuroendocrine Effects of the Chronic Stress Paradigm

A schematic diagram of the experimental design is given in Fig. 1a. Briefly, three different stressors (i.e., exposure to rat, restraint stress, and tail suspension stress) were applied in an alternating fashion over the course of the experiment. Chronically stressed mice (CS) gained significantly less weight than control animals (C), which were left unperturbed in their home cages (Fig. 1b). Adrenal weight was significantly increased in CS mice after completion of the stress paradigm (Fig. 1c, d). Acute stress, i.e., a single session of exposure to rat before sacrifice early on the following morning, resulted in significantly increased circulating corticosterone levels and no relevant change in adrenal gland weight relative to C mice (Fig. 1c, e). By contrast, CS mice showed significantly reduced corticosterone plasma concentrations relative to C mice at the end of the experiment (Fig. 1e). Next, we studied mRNA transcription of genes associated with corticosteroid signaling in the left hypothalamus (Fig. 1f). Expression of glucocorticoid receptor (*Nr3c1*) mRNA and expression of mineralocorticoid receptor (*Nr3c2*) mRNA did not differ significantly between C and CS mice. However, CS mice showed significantly increased mRNA transcription of *Fkbp5* and *Crh* (Fig. 1f). Further, Western blot analysis of homogenates prepared from right hypothalamus confirmed increased FKBP5 protein expression in CS mice (Fig. 1g, h).

## Chronic Stress Impacts the Brain's Sensitivity to Ischemic Injury

Next, we combined the chronic stress procedure with a model of mild transient brain ischemia (Fig. 2a). C and CS mice were used. Two days after 30 min MCAo/reperfusion, lesion size was measured in vivo using T2-weighted MRI. Lesion volume was found to be significantly increased in CS mice compared to C mice (Fig. 2b). Endothelial mechanisms have been implicated in linking psychological stress with stroke vulnerability [13, 14]. We therefore performed a gene expression analysis using ex vivo ECs harvested separately from the ischemic MCA territory and the corresponding area in the contralateral non-ischemic hemisphere (Fig. 2c). C and CS samples were pooled from groups of 3–5 mice (Fig. 2c). As illustrated in Fig. 2d, cells pre-enriched for CD31 were FACS purified to obtain CD45-/DAPI-/CD31+/CD146+ brain endothelia. An analysis of cell type-specific genes confirmed the purity of the FAC-sorted cells (Fig. 2e). Finally, a principal component analysis (PCA) performed on the RNA-seq data yielded two factors (Fig. 2f).

## A Transcriptomic Signature of Chronic Stress in MCAo-Exposed Endothelium

Volcano plots show genes that were increased or decreased by more than two-fold ($p < 0.05$) in ipsilateral compared to contralateral endothelium (Fig. 3a, b). The number of differentially expressed genes (DEGs) was higher in endothelia from CS mice than in endothelia from C mice. Figure 3c summarizes the number of DEGs in C and CS mice as well as the intersection of genes regulated similarly in both experimental groups. A complete list of genes included in each category is provided in supplementary material ESM 2–4. Additionally, Fig. 3d summarizes the number of DEGs in different log2 (fold change) categories. RNA-seq did not yield differences in gene expression between ECs harvested from the contralateral hemisphere of C mice and ECs harvested from the contralateral hemisphere of CS mice.

Next, we performed a GO term analysis for the DEGs in each group. The annotation rates of the DEGs were 84.9% and 96.3% in ECs from C and CS mice, respectively. ESM 1a summarizes biological process GO terms that were simultaneously enriched in ECs from both C and CS mice ($p < 0.01$). Additional biological process GO terms emerged in CS mice. The top 10 of these terms are given in Fig. 3e. The biological processes in question are highly relevant to endothelial viability and function and highlight the effects of prior stress priming on the transcriptomic response to MCAo. The complete lists of GO terms enriched exclusively in C or CS mice are given in ESM 1b and 1c.

**Fig. 2** Chronic stress increases early lesion size after MCAo. **a** ▶ Experimental setup. Animals were either subjected to the 28-day stress procedure (CS) or were left unperturbed (C). On day 29, C and CS mice underwent 30 min MCAo/reperfusion. Successful MCAo was confirmed at 48 h by T2-weighted MRI. Mice were sacrificed 72 h after MCAo. **b** Chronic stress resulted in increased acute lesion sizes after 30 min MCAo. C: $n = 25$, CS: $n = 26$. Mann-Whitney $U$ test. $U = 213$, $*p < 0.05$. **c**, **d** Endothelial cells (ECs) were harvested from the ipsilateral (ipsi; i.e., infarcted MCA territory) and contralateral (contra; i.e., corresponding area on the non-infarcted side) hemispheres of C and CS mice. Cells from 3–5 mice were pooled for each sample. **d** Gating strategy for flow cytometric sorting of MACS-purified CD31+ cells. **e** The heatmap confirms strong expression of endothelial marker genes in all samples. **f** Principal component analysis (PCA) plot of all RNA-seq data. The two-dimensional scatter plot represents the differential patterns of gene expression in ECs harvested from C and CS mice after 30 min MCAo/reperfusion. FPKM, fragments per kilobase per million fragments mapped

## Upregulation of MicroRNA-34a Promotes Ischemic Injury

MicroRNA-34a is increased by atheroprone oscillatory shear stress and promotes endothelial senescence [36, 37]. MiR-34a has previously been shown to repress SIRT1 expression [37, 38]. MiR-34a-5p and miR-34a-3p are the mature sequences of miR-34a.

MiR-34a was one of the transcripts found to be only differentially regulated in ECs from CS mice (Fig. 3b). Crucially, miR-34a was associated with nine of the top 10 biological process GO terms exclusively enriched in CS endothelium (Fig. 3e). We therefore investigated the relationship between expression of mature miR-34a-5p and miR-34a-3p in ischemic brain tissue and MRI lesion size.

There was considerable variance in infarct size among mice in the CS group, possibly reflecting partial resilience to the adverse effects of chronic stress in a subgroup of CS mice. For this reason, we divided CS mice into two groups based on their infarct sizes: (1) 'CS large' group with an infarct size above the median of the CS group, (2) 'CS small' group. Expression of miR-34a-5p and miR-34a-3p was significantly increased while *Sirt1* mRNA expression was significantly decreased in the 'CS large' group relative to both the 'CS small' group and C mice (Fig. 4a–c). Interestingly, mRNA transcription of *Fkbp5* observed from ischemic whole brain tissue did not differ significantly between experimental groups (Fig. 4d). However, we still found a moderate positive relationship between mRNA transcription of *Fkbp5* in ischemic brain tissue and infarct volume (Fig. 4e).

Expression of miR-34a-5p and miR-34a-3p was positively related to infarct size (Fig. 4f, g) and negatively related to *Sirt1* mRNA expression (Fig. 4h, i). Finally, transcription of *Sirt1* mRNA was negatively related to the size of the ischemic lesion (Fig. 4j).

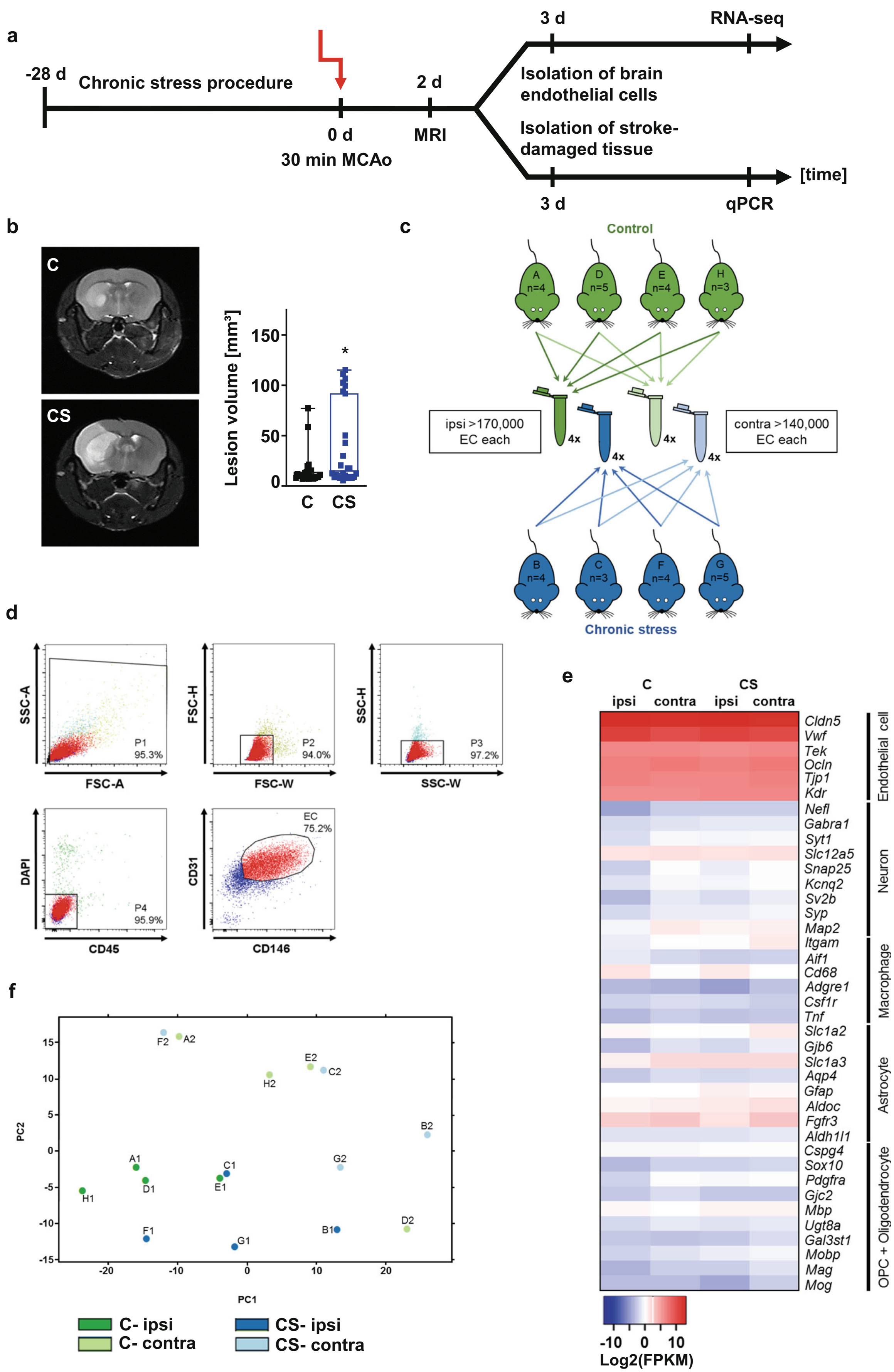

a
-28 d
Chronic stress procedure
0 d
30 min MCAo
2 d
MRI
3 d
RNA-seq
Isolation of brain endothelial cells
Isolation of stroke-damaged tissue
3 d
qPCR
[time]
b
C
CS
Lesion volume [mm³]
c
Control
ipsi >170,000 EC each
contra >140,000 EC each
Chronic stress
d
SSC-A
FSC-A
FSC-H
FSC-W
SSC-H
SSC-W
DAPI
CD45
CD31
CD146
EC 75.2%
e
C
CS
ipsi
contra
Endothelial cell
Neuron
Macrophage
Astrocyte
OPC + Oligodendrocyte
Cldn5
Vwf
Tek
Ocln
Tjp1
Kdr
Nefl
Gabra1
Syt1
Slc12a5
Snap25
Kcnq2
Sv2b
Syp
Map2
Itgam
Aif1
Cd68
Adgre1
Csf1r
Tnf
Slc1a2
Gjb6
Slc1a3
Aqp4
Gfap
Aldoc
Fgfr3
Aldh1l1
Cspg4
Sox10
Pdgfra
Gjc2
Mbp
Ugt8a
Gal3st1
Mobp
Mag
Mog
Log2(FPKM)
f
PC1
PC2
C- ipsi
C- contra
CS- ipsi
CS- contra

## Discussion

While this study focuses chiefly on endothelial mechanisms, it is noted that the adverse effects of chronic stress are far-reaching and clearly not restricted to a single cell type in the brain. For example, the expression of neurotrophins in brain tissue is strongly impacted by stress and corticosteroids, which, in turn, may affect cellular plasticity and neuronal vulnerability to ischemia [39, 40]. With this being acknowledged, however, one key advantage to our reductionist approach is that it provides a new and hitherto barely considered angle on the complex pathways linking stress and stroke.

This study yielded the following key findings: (1) The chronic stress paradigm exerted robust effects at multiple levels, including, among others, reduced weight gain, increased adrenal gland weight, and increased hypothalamic FKBP5 mRNA and protein expression. (2) Using T2-weighted MR imaging, we replicate our earlier finding that the chronic stress paradigm sensitizes experimental animals to the effects of 30 min MCAo/reperfusion. (3) Next, we used RNA sequencing to profile gene expression changes in endothelia harvested from the ischemic brain as an effect of prior stress. We identified a distinct transcriptomic signature characterized by a higher number of DEGs in MCAo-exposed ECs derived from CS mice. Biological process GO terms enriched in ECs from CS mice are highly relevant to cell viability and function and include terms such as "cell proliferation," "negative regulation of biological process," "positive regulation of apoptotic process," "cell death," "negative regulation of signal transduction," and "negative regulation of cell proliferation." MicroRNA-34a is associated with nine of the top 10 biological process GO terms enriched in CS endothelium. (4) Expression of mature miR-34a-5p and miR-34a-3p in ischemic brain tissue was positively related to infarct size measured by MRI and negatively related to *Sirt1* mRNA expression.

Both reduced body weight [16, 41, 42] and increased body weight [43–45] have been observed with different rodent stress models. Factors that may explain differences between studies include the age, sex, and strain of the experimental animals, the kind of stressor used, and, importantly, the duration of the stressor [45, 46]. The chronic stress model was initially developed by Strekalova et al. with a view to producing a depression-like syndrome in male C57BL/6 mice [16]. For stroke experiments, our group adapted this model to 129S6/SvEv mice [13, 14], which, because of the nature of their cerebrovascular anatomy, lend themselves particularly well to transient intraluminal MCAo [47]. Our finding of reduced body weight in CS mice relative to non-stressed controls is in accord with the initial report by Strekalova et al. [16]. In line with our earlier study [13], the present investigation also confirms dysregulation of the HPA axis in the form of increased adrenal glands in CS mice. Furthermore, we show here that, in our model, chronic stress leads to

**Fig. 3** Transcriptomic analysis of brain ECs. ECs were harvested from C ▶ and CS mice 72 h after 30 min MCAo. Upregulation or downregulation of gene expression is relative to gene expression in endothelia harvested from the contralateral hemisphere. **a**, **b** Volcano plots of all genes quantified by RNA-seq. The negative log10 of the *p* value is plotted on the *y* axis. The *x* axis is the log2 of the fold change between endothelial gene expression in the ipsilateral and contralateral sides. **a** Gene expression in control (C) animals. **b** Gene expression in chronically stressed mice (CS). Green dots represent genes which are significantly upregulated or downregulated in C mice. Blue dots represent genes which are significantly upregulated or downregulated in CS mice. Yellow dots represent genes significantly regulated in both C and CS mice. Gray dots represent genes without significant regulation. The two vertical columns of pink dots in the chart are genes for which no expression was detected in ECs harvested from either the contralateral or the ipsilateral hemisphere, so log2(fold change) values were arbitrarily set to ± 20 (instead of ± infinity). Note that genes with a log2(fold change) value of infinity and FDR < 0.05 were not considered as differentially expressed due to low mean read counts. **c** Venn diagram showing the number and overlap of differentially regulated genes in ECs from C and CS mice. Green circle: endothelial gene expression in C mice; blue circle: endothelial gene expression in CS mice. **d** The table summarizes the number of differentially expressed genes (DEGs) in different log2(fold change) categories. **e** The top 10 biological process GO terms that were only detected in CS mice (see supplementary data for entire list)

upregulation of both *Crh* mRNA and FKBP5 mRNA and protein in hypothalamus. FKBP5 mRNA and protein expression is induced upon glucocorticoid receptor stimulation, providing an intracellular negative feedback loop for glucocorticoid receptor activity [48]. Together, these results strongly point to depression-like HPA axis hyperactivity and glucocorticoid resistance in mice subjected to 4 weeks of chronic stress [49, 50]. Interestingly, measurements in morning plasma performed at the end of the stress regime revealed decreased corticosterone concentrations in CS mice. A similar result has previously been reported in a chronic social defeat paradigm [45]. As plasma was taken 1 day after the end of the stress procedure and the animals had been left undisturbed in their home cages during the preceding dark phase, reduced trough corticosterone levels in CS mice most likely reflect adaptive changes of the HPA axis to chronic stress [45].

In the current study, we used the MCAo model to apply a cell-specific transcriptomic approach to uncover stress signatures in cerebrovascular endothelium. In doing so, we focused on molecular and physiological endpoints along with early lesion size on MRI. To our knowledge, this is the first report investigating the effects of chronic psychological stress on the endothelial transcriptome. Expression profiling of cerebrovascular endothelium following MCAo has likewise not yet been reported in the literature.

After completion of the 4-week chronic stress procedure, experimental mice were subjected to 30 min MCAo/reperfusion and sacrificed after an interval of 72 h. Our results, therefore, reflect the enduring effects of prior stress on stroke outcome. We acknowledge that our study does not address the connection between

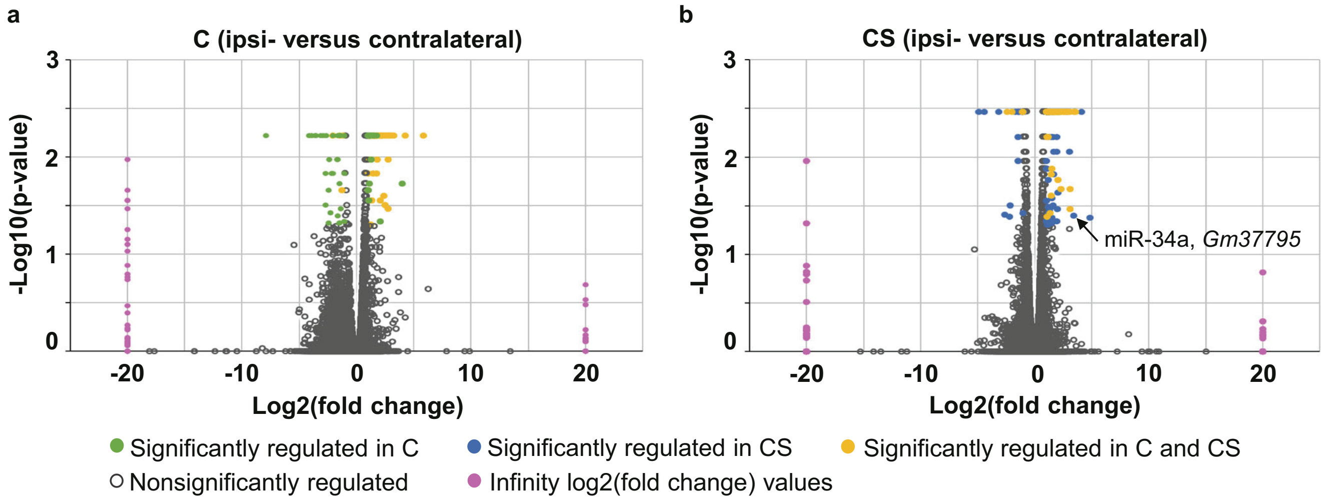


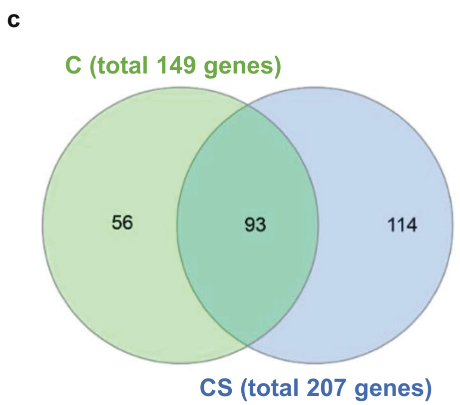


d

| | C | CS |
|---|---|---|
| **Log2(fold change) induction** | **Number of DEGs** | **Number of DEGs** |
| ≥ 1 < 2 | 83 | 134 |
| ≥ 2 < 3 | 26 | 32 |
| ≥ 3 < 4 | 3 | 9 |
| ≥ 4 < 5 | 1 | 2 |
| ≥ 5 < 6 | 1 | 0 |
| ≥ 6 < 7 | 0 | 0 |
| ≥ 7 < 8 | 0 | 0 |
| ≥ 8 | 0 | 0 |
| **Log2(fold change) reduction** | **Number of DEGs** | **Number of DEGs** |
| ≥ 1 < 2 | 17 | 22 |
| ≥ 2 < 3 | 12 | 5 |
| ≥ 3 < 4 | 4 | 1 |
| ≥ 4 < 5 | 1 | 2 |
| ≥ 5 < 6 | 0 | 0 |
| ≥ 6 < 7 | 0 | 0 |
| ≥ 7 < 8 | 1 | 0 |
| ≥ 8 | 0 | 0 |

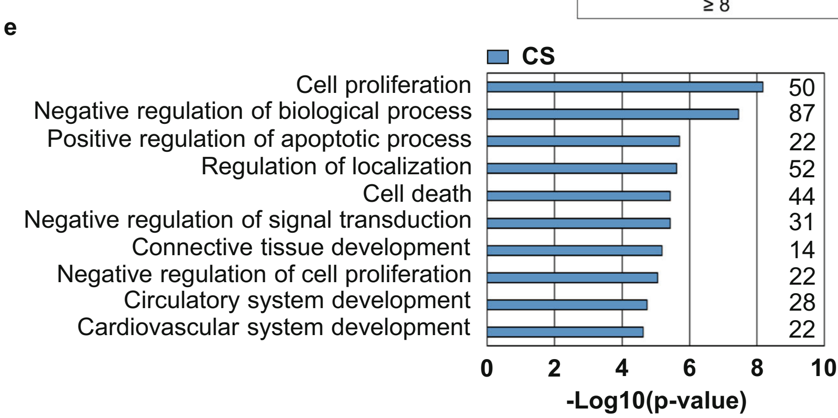


chronic stress, depressive-like behaviors, and functional outcomes after transient brain ischemia. However, in agreement with earlier studies using histological evaluation of infarct size [12–14, 51], T2-weighted imaging at 48 h confirmed a stress-induced increase in lesion volume.

ECs were isolated from the ipsilateral and contralateral MCA territory using sequential rounds of MACS and FACS. First, ECs were enriched by CD31 magnetic beads. Then, progressive FACS gating was used to remove cellular aggregates and cellular debris, as well as CD31 expressing hematopoietic cells [52, 53]. Purity of ECs was corroborated by robust expression of endothelial cell-specific marker genes alongside the absence of marker genes for other brain cells. Interestingly, we did not detect significant differences in gene expression

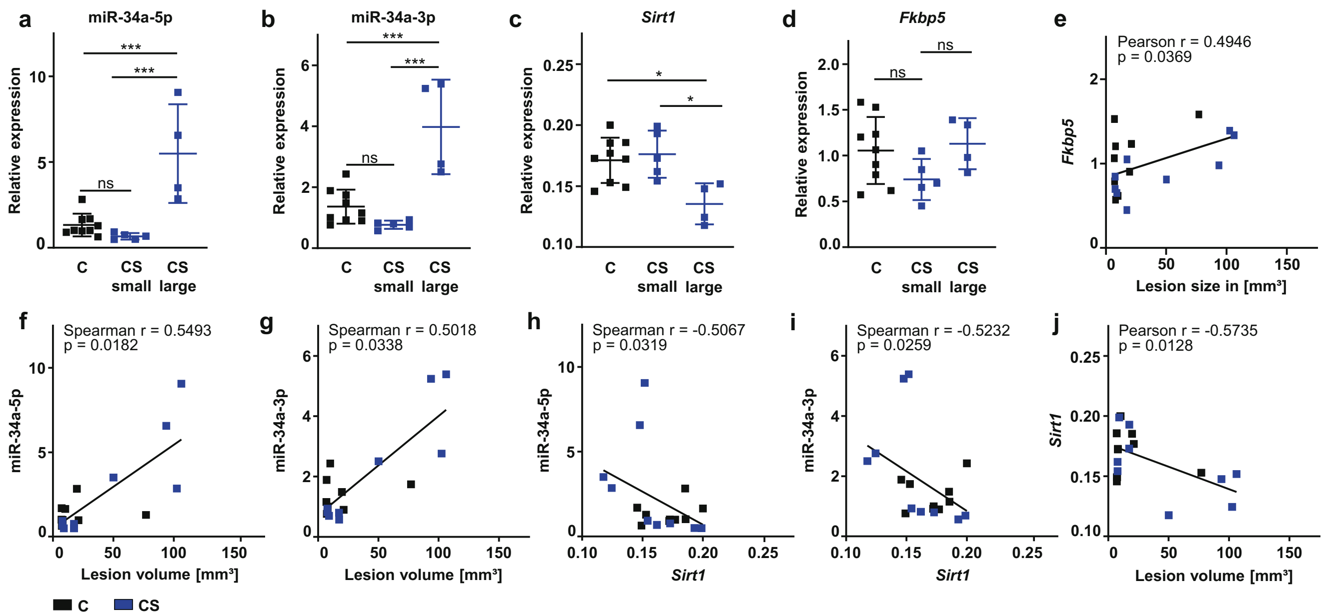


**Fig. 4** Expression of miR-34a microRNAs is positively related to lesion size and inversely related to *Sirt1* mRNA expression in ischemic whole brain. Mice were killed 72 h after 30 min MCAo/reperfusion. As described in the main text, CS mice were divided into two groups based on their infarct sizes—'CS large' group and 'CS small' group. Expression levels of miR-34a-5p, miR-34a-3p, *Sirt1*, and *Fkbp5* were assessed in ischemic whole brain tissue. MiR-34a values are expressed as fold change relative to RNU6B and one control mouse using the $2^{(-\Delta\Delta Ct)}$ method. Relative *Sirt1* and *Fkbp5* mRNA expression values were calculated using the ΔCT method corrected for primer efficiency and normalized to *Tpp2* as housekeeping gene. **a**–**d** C: $n = 9$, 'CS small' group: $n = 5$, 'CS large' group: $n = 4$. **e**–**j** $N = 9$ mice per group. **a** One-way ANOVA $F(2,15) = 16.28$, $p < 0.001$ with Tukey's multiple comparison test: ***$p < 0.001$. **b** One-way ANOVA $F(2,15) = 19.82$, $p < 0.001$ with Tukey's multiple comparison test: ***$p < 0.001$. **c** One-way ANOVA $F(2,15) = 6.575$, $p < 0.01$ with Tukey's multiple comparison test: *$p < 0.05$. **d** One-way ANOVA $F(2,15) = 2.138$, $p = 0.152$. **e**–**j** Pearson's correlation coefficient or Spearman's rank correlations were computed depending on whether data were normally distributed or not

between ECs harvested from the contralateral hemispheres of C and CS mice. This most likely suggests that, in our experimental setup, the 3-day interval between stress and sacrifice was too long for the effects of psychological stress to persist on the transcriptomic level in otherwise unperturbed brain endothelium. Of course, the effects of the intervening MCAo also have to be taken into consideration as the procedure itself is

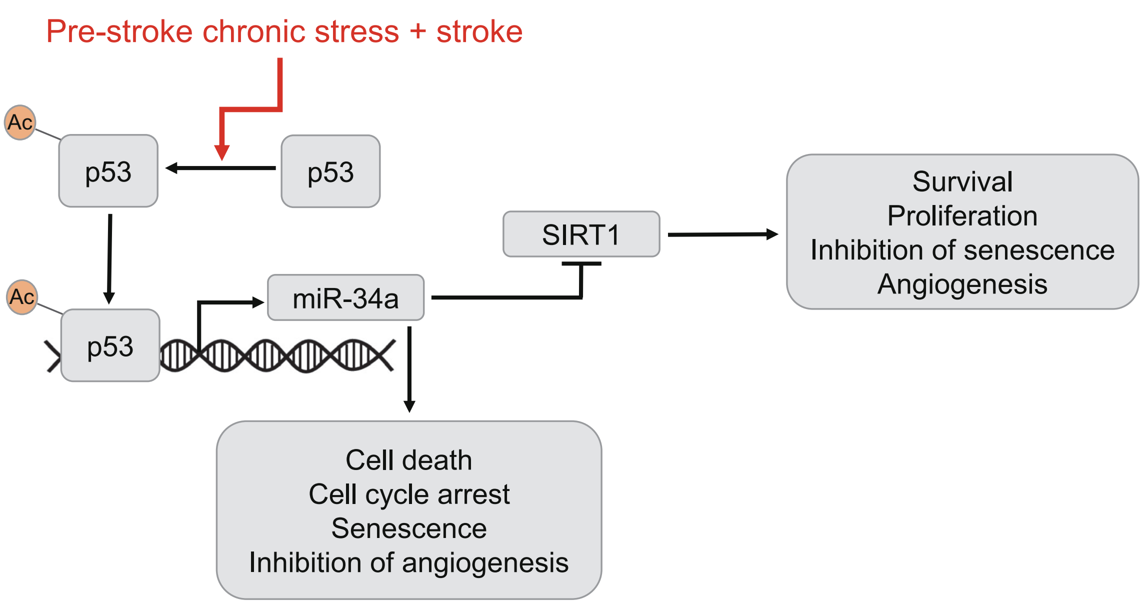


**Fig. 5** Upregulation of miR-34a in brain endothelia of CS mice after MCAo. The combination of ischemic injury and chronic stress results in increased transcriptional activity of p53, most likely through a posttranslational modification such as increased acetylation [38]. In consequence, miR-34a is upregulated, resulting in repression of SIRT1 and modulation of proliferation and apoptosis [37, 38]

a strong stressor and leads to elevations in circulating corticosterone [e.g., 54].

In this analysis, we focused on genes that were either increased or decreased by more than two-fold ($p < 0.05$) in ipsilateral compared to contralateral ECs. As can be seen from the Volcano plots in Fig. 3, relatively few transcripts fell into this category. Biological process GO terms enriched in both C and CS mice are summarized in ESM 1a and reflect the broad cellular effects of ischemia on ECs. As described above, more DEGs were detected in CS than in C mice. Further exploration of our genomic findings will prove useful in elucidating the adverse effects of stress on ECs in the pathogenesis of stroke. For example, the upregulation of *Angpt2* in CS mice may point to altered blood vessel growth in the ischemic brain as angiopoietin-2 has been shown to impair revascularization after limb ischemia [55]. *Adamts9*, which was similarly upregulated in ipsilateral CS endothelium, has recently been identified as an endogenous angiogenesis inhibitor that operates cell-autonomously in ECs [56]. By contrast, mRNA expression of the brain-specific angiogenesis inhibitor 1 (*Adgrb1*) was not altered in CS endothelium, but strongly downregulated in ipsilateral ECs from C mice [57]. In the context of these observations, it is important to note that endothelial cell proliferation and angiogenesis are crucial regenerative mechanisms post-stroke [e.g., 58–61].

Finally, microRNA-34a was selectively increased in CS endothelium from the ischemic brain. This finding is highly significant in the context of a confluence of research pointing to the importance of vascular mechanisms and regenerative angiogenesis for stroke outcome [58, 62, 63]. We speculate that pre-stroke stress in tandem with stroke injury enhances transcriptional activity of p53 most likely through its acetylation [38]. In turn, acetylated p53 upregulates miR-34a, thereby repressing SIRT1 and modulating proliferation and apoptosis [37, 38]. A schema of the putative underlying miR-34a pathway in brain endothelia is presented in Fig. 5.

There is ample evidence in the literature to indicate that changes in miR-34a and miR-34a target genes such as *Sirt1* will directly impact ischemic injury and, hence, infarct size. MiR-34a has been identified as a key driver of cardiovascular senescence [37, 64]. Moreover, anti-miR34a treatment following experimental myocardial infarction (MI) via coronary artery ligation significantly improved cardiac function post-MI [65]. Expression of miR-34a is elevated in senescent human umbilical cord vein endothelial cells as well as in heart and spleen of older mice [37]. MiR-34a induces G1 arrest, thereby blocking endothelial cell proliferation [37]. Conversely, inhibition of miR-34a by antisense oligonucleotides has been shown to increase capillary density in a mouse model of myocardial infarction, highlighting the favorable effects of inhibition of miR-34a on cardiac endothelium in the ischemic border zone [64]. Finally, SIRT1 is expressed by vascular endothelium in brain and has been shown to mediate cerebrovascular protection by facilitating NO-dependent vascular relaxation in a murine model of cerebral hypoperfusion induced by bilateral common carotid artery stenosis [66]. A growing body of evidence suggests that miRNAs may be released into the bloodstream or cerebrospinal fluid (CSF), making them attractive candidates for biomarker development. It is, therefore, especially notable that exciting new research has reported increased miR-34a-5p concentrations in blood and CSF of patients suffering from major depression [67]. Due to limited EC numbers, 3 to 5 samples per experimental condition had to be pooled in the current study. For this reason, it was not possible to directly correlate endothelial miR-34a expression to infarct size. However, in a subsequent experiment, we examined the relationship between MRI lesion size and expression of mature miR-34a-5p and miR-34a-3p in ischemic whole brain tissue. SIRT1 expression has been shown to be repressed by miR-34a [38]. Our analysis shows that expression of miR-34a-5p and miR-34a-3p was positively related to infarct size whereas *Sirt1* transcription was negatively related to infarct size. An obvious caveat to this finding is that miR-34a may be expressed by neurons as well as by other non-neuronal cells besides endothelia [68, 69].

In conclusion, this study identifies a transcriptomic signature of chronic stress in endothelia harvested from the ischemic murine brain. This stress signature relates to worse stroke outcome and is directly relevant to endothelial mechanisms in the pathogenesis of stroke.

**Acknowledgments** The technical assistance of Bettina Herrmann, Melanie Kroh, Renate Franke, and Stefanie Balz is gratefully acknowledged. We also thank the Charité Core Facility '7T Experimental MRIs' and the Deutsches Rheuma-Forschungszentrum Berlin 'Flow Cytometry Core Facility' (FCCF) for excellent support.

**Funding Information** This work was supported by the Deutsche Forschungsgemeinschaft (Exc257 to M.E.; KR 2956/4-1 und KR 2956/6-1 to G.K.; GE 2576/3-1 und GE 2576/5-1 to K.G.), the Bundesministerium für Bildung und Forschung (CSB to M.E., K.G. and G.K.), the German Center for Neurodegenerative Diseases (DZNE to M.E.), the German Center for Cardiovascular Research (DZHK to M.E. and K.G.), and the Corona Foundation (to M.E.).

## Compliance with Ethical Standards

**Conflict of Interest** The authors declare that they have no competing interests.



## References

1. Rosengren A, Hawken S, Ounpuu S, Sliwa K, Zubaid M, Almahmeed WA, Blackett KN, Sitthi-amorn C et al (2004) Association of psychosocial risk factors with risk of acute

myocardial infarction in 11119 cases and 13648 controls from 52 countries (the INTERHEART study): case-control study. Lancet. 364:953–962
2. O'Donnell MJ, Xavier D, Liu L, Zhang H, Chin SL, Rao-Melacini P et al (2010) Risk factors for ischaemic and intracerebral haemorrhagic stroke in 22 countries (the INTERSTROKE study): A case-control study. Lancet. 376:112–123
3. Everson-Rose SA, Roetker NS, Lutsey PL, Kershaw KN, Longstreth WT, Sacco RL et al (2014) Chronic stress, depressive symptoms, anger, hostility, and risk of stroke and transient ischemic attack in the multi-ethnic study of atherosclerosis. Stroke. 45:2318–2323
4. Kershaw KN, Lane-Cordova AD, Carnethon MR, Tindle HA, Liu K (2017) Chronic stress and endothelial dysfunction: the multi-ethnic study of atherosclerosis (MESA). Am J Hypertens 30:75–80
5. Mausbach BT, Roepke SK, Ziegler MG, Milic M, von Känel R, Dimsdale JE et al (2010) Association between chronic caregiving stress and impaired endothelial function in the elderly. J Am Coll Cardiol 55:2599–2606
6. Ghiadoni L, Donald AE, Cropley M, Mullen MJ, Oakley G, Taylor M, O'Connor G, Betteridge J et al (2000) Mental stress induces transient endothelial dysfunction in humans. Circulation. 102: 2473–2478
7. Spieker LE, Hürlimann D, Ruschitzka F, Corti R, Enseleit F, Shaw S, Hayoz D, Deanfield JE et al (2002) Mental stress induces prolonged endothelial dysfunction via endothelin-A receptors. Circulation. 105:2817–2820
8. Broadley AJM, Korszun A, Abdelaal E, Moskvina V, Jones CJH, Nash GB, Ray C, Deanfield J et al (2005) Inhibition of cortisol production with metyrapone prevents mental stress-induced endothelial dysfunction and baroreflex impairment. J Am Coll Cardiol 46:344–350
9. Eriksson M, Johansson K, Sarabi M, Lind L (2007) Mental stress impairs endothelial vasodilatory function by a beta-adrenergic mechanism. Endothelium. 14:151–156
10. Hijmering ML, Stroes ESG, Olijhoek J, Hutten BA, Blankestijn PJ, Rabelink TJ (2002) Sympathetic activation markedly reduces endothelium-dependent, flow-mediated vasodilation. J Am Coll Cardiol 39:683–688
11. DeVries AC, Joh H-D, Bernard O, Hattori K, Hurn PD, Traystman RJ, Alkayed NJ (2001) Social stress exacerbates stroke outcome by suppressing Bcl-2 expression. Proc Natl Acad Sci U S A 98:11824–11828
12. Sugo N, Hurn PD, Morahan MB, Hattori K, Traystman RJ, DeVries AC (2002) Social stress exacerbates focal cerebral ischemia in mice. Stroke. 33:1660–1664
13. Balkaya M, Prinz V, Custodis F, Gertz K, Kronenberg G, Kroeber J, Fink K, Plehm R et al (2011) Stress worsens endothelial function and ischemic stroke via glucocorticoids. Stroke. 42:3258–3264
14. Custodis F, Gertz K, Balkaya M, Prinz V, Mathar I, Stamm C, Kronenberg G, Kazakov A et al (2011) Heart rate contributes to the vascular effects of chronic mental stress: effects on endothelial function and ischemic brain injury in mice. Stroke. 42:1742–1749
15. Kilkenny C, Browne WJ, Cuthill IC, Emerson M, Altman DG (2010) Improving bioscience research reporting: the ARRIVE guidelines for reporting animal research. PLoS Biol 8:e1000412
16. Strekalova T, Spanagel R, Bartsch D, Henn FA, Gass P (2004) Stress-induced anhedonia in mice is associated with deficits in forced swimming and exploration. Neuropsychopharmacology. 29:2007–2017
17. Gerriets T, Stolz E, Walberer M, Müller C, Kluge A, Bachmann A et al (2004) Noninvasive quantification of brain edema and the space-occupying effect in rat stroke models using magnetic resonance imaging. Stroke. 35:566–571
18. Nishida Y, Sugahara-Kobayashi M, Takahashi Y, Nagata T, Ishikawa K, Asai S (2006) Screening for control genes in mouse hippocampus after transient forebrain ischemia using high-density oligonucleotide array. J Pharmacol Sci 101:52–57
19. Livak KJ, Schmittgen TD (2001) Analysis of relative gene expression data using real-time quantitative PCR and the 2(-Delta Delta C(T)) Method. Methods. 25:402–408
20. Schmieder R, Lim YW, Edwards R (2012) Identification and removal of ribosomal RNA sequences from metatranscriptomes. Bioinformatics. 28:433–435
21. Edgar R, Domrachev M, Lash AE (2002) Gene Expression Omnibus: NCBI gene expression and hybridization array data repository. Nucleic Acids Res 30:207–210
22. Dobin A, Davis CA, Schlesinger F, Drenkow J, Zaleski C, Jha S, Batut P, Chaisson M et al (2013) STAR: ultrafast universal RNA-seq aligner. Bioinformatics. 29:15–21
23. Anders S, Pyl PT, Huber W (2015) HTSeq - a Python framework to work with high-throughput sequencing data. Bioinformatics. 31: 166–169
24. Heberle H, Vaz Meirelles G, da Silva FR, Telles GP, Minghim R (2015) InteractiVenn: a web-based tool for the analysis of sets through Venn diagrams. BMC Bioinformatics 16:169
25. Babicki S, Arndt D, Marcu A, Liang Y, Grant JR, Maciejewski A et al (2016) Heatmapper: web-enabled heat mapping for all. Nucleic Acids Res 44(Web Server):W147–W153
26. Cahoy JD, Emery B, Kaushal A, Foo LC, Zamanian JL, Christopherson KS et al (2008) A transcriptome database for astrocytes, neurons, and oligodendrocytes: a new resource for understanding brain development and function. J Neurosci 28:264–278
27. Wiedenmann B, Franke WW (1985) Identification and localization of synaptophysin, an integral membrane glycoprotein of Mr 38,000 characteristic of presynaptic vesicles. Cell. 41:1017–1028
28. Dinsmore JH, Solomon F (1991) Inhibition of MAP2 expression affects both morphological and cell division phenotypes of neuronal differentiation. Cell. 64:817–826
29. Chawla A, Barak Y, Nagy L, Liao D, Tontonoz P, Evans RM (2001) PPAR-$\gamma$ dependent and independent effects on macrophage-gene expression in lipid metabolism and inflammation. Nat Med 7:48–52
30. Ito D, Imai Y, Ohsawa K, Nakajima K, Fukuuchi Y, Kohsaka S (1998) Microglia-specific localisation of a novel calcium binding protein, Iba1. Brain Res Mol Brain Res 57:1–9
31. Zakrzewska A, Cui C, Stockhammer OW, Benard EL, Spaink HP, Meijer AH (2010) Macrophage-specific gene functions in Spi1-directed innate immunity. Blood. 116:e1–e11
32. Mustonen T, Alitalo K (1995) Endothelial receptor tyrosine kinases involved in angiogenesis. J Cell Biol 129:895–898
33. Stevenson BR, Siliciano JD, Mooseker MS, Goodenough DA (1986) Identification of ZO-1: a high molecular weight polypeptide associated with tight junction (zonula occludens) in a variety of epithelia. J Cell Biol 103:755–766
34. Reimand J, Arak T, Adler P, Kolberg L, Reisberg S, Peterson H et al (2016) g:Profiler-a web server for functional interpretation of gene lists (2016 update). Nucleic Acids Res 44(Web Server):W83–W89
35. Supek F, Bošnjak M, Škunca N, Šmuc T (2011) REVIGO summarizes and visualizes long lists of gene ontology terms. PLoS One 6: e21800
36. Fan W, Fang R, Wu X, Liu J, Feng M, Dai G, Chen G, Wu G (2015) Shear-sensitive microRNA-34a modulates flow-dependent regulation of endothelial inflammation. J Cell Sci 128:70–80
37. Ito T, Yagi S, Yamakuchi M (2010) MicroRNA-34a regulation of endothelial senescence. Biochem Biophys Res Commun 398:735–740
38. Yamakuchi M, Ferlito M, Lowenstein CJ (2008) miR-34a repression of SIRT1 regulates apoptosis. Proc Natl Acad Sci U S A 105: 13421–13426
39. Smith MA, Makino S, Kvetnansky R, Post RM (1995) Stress and glucocorticoids affect the expression of brain-derived neurotrophic

factor and neurotrophin-3 mRNAs in the hippocampus. J Neurosci 15:1768–1777
40. Endres M, Fan G, Hirt L, Fujii M, Matsushita K, Liu X, Jaenisch R, Moskowitz MA (2000) Ischemic brain damage in mice after selectively modifying BDNF or NT4 gene expression. J Cereb Blood Flow Metab 20:139–144
41. Magariños AM, McEwen BS (1995) Stress-induced atrophy of apical dendrites of hippocampal CA3c neurons: involvement of glucocorticoid secretion and excitatory amino acid receptors. Neuroscience. 69:89–98
42. Warren BL, Vialou VF, Iñiguez SD, Alcantara LF, Wright KN, Feng J, Kennedy PJ, Laplant Q et al (2013) Neurobiological sequelae of witnessing stressful events in adult mice. Biol Psychiatry 73: 7–14
43. Hammamieh R, Chakraborty N, De Lima TCM, Meyerhoff J, Gautam A, Muhie S et al (2012) Murine model of repeated exposures to conspecific trained aggressors simulates features of post-traumatic stress disorder. Behav Brain Res 235:55–66
44. Patterson ZR, Khazall R, MacKay H, Anisman H, Abizaid A (2013) Central ghrelin signaling mediates the metabolic response of C57BL/6 male mice to chronic social defeat stress. Endocrinology. 154:1080–1091
45. Savignac HM, Finger BC, Pizzo RC, O'Leary OF, Dinan TG, Cryan JF (2011) Increased sensitivity to the effects of chronic social defeat stress in an innately anxious mouse strain. Neuroscience. 192:524–536
46. Sutanto W, de Kloet ER (1994) The use of various animal models in the study of stress and stress-related phenomena. Lab Anim 28: 293–306
47. Maeda K, Hata R, Hossmann K-A (1998) Differences in the cerebrovascular anatomy of C57Black/6 and SV129 mice. Neuroreport. 9:1317–1319
48. Binder EB (2009) The role of FKBP5, a co-chaperone of the glucocorticoid receptor in the pathogenesis and therapy of affective and anxiety disorders. Psychoneuroendocrinology. 34(Suppl 1): S186–S195
49. Westberry JM, Sadosky PW, Hubler TR, Gross KL, Scammell JG (2006) Glucocorticoid resistance in squirrel monkeys results from a combination of a transcriptionally incompetent glucocorticoid receptor and overexpression of the glucocorticoid receptor co-chaperone FKBP51. J Steroid Biochem Mol Biol 100:34–41
50. Pariante CM, Miller AH (2001) Glucocorticoid receptors in major depression: relevance to pathophysiology and treatment. Biol Psychiatry 49:391–404
51. Madrigal JLM, Caso JR, de Cristóbal J, Cárdenas A, Leza JC, Lizasoain I, Lorenzo P, Moro MA (2003) Effect of subacute and chronic immobilisation stress on the outcome of permanent focal cerebral ischaemia in rats. Brain Res 979:137–145
52. Kim S-J, Kim J-S, Papadopoulos J, Wook Kim S, Maya M, Zhang F, He J, Fan D et al (2009) Circulating monocytes expressing CD31: implications for acute and chronic angiogenesis. Am J Pathol 174:1972–1980
53. Wilkinson R, Lyons BA, Roberts D, Wong M-X, Bartley PA, Jackson DE (2002) Platelet endothelial cell adhesion molecule-1 (PECAM-1/CD31) acts as a regulator of B-cell development, B-cell antigen receptor (BCR)-mediated activation, and autoimmune disease. Blood. 100:184–193
54. Becker KJ, McCarron RM, Ruetzler C, Laban O, Sternberg E, Flanders KC, Hallenbeck JM (1997) Immunologic tolerance to myelin basic protein decreases stroke size after transient focal cerebral ischemia. Proc Natl Acad Sci U S A 94:10873–10878
55. Reiss Y, Droste J, Heil M, Tribulova S, Schmidt MHH, Schaper W, Dumont DJ, Plate KH (2007) Angiopoietin-2 impairs revascularization after limb ischemia. Circ Res 101:88–96
56. Koo B-H, Coe DM, Dixon LJ, Somerville RPT, Nelson CM, Wang LW, Young ME, Lindner DJ et al (2010) ADAMTS9 is a cell-autonomously acting, anti-angiogenic metalloprotease expressed by microvascular endothelial cells. Am J Pathol 176:1494–1504
57. Nishimori H, Shiratsuchi T, Urano T, Kimura Y, Kiyono K, Tatsumi K et al (1997) A novel brain-specific p53-target gene, BAI1, containing thrombospondin type 1 repeats inhibits experimental angiogenesis. Oncogene. 15:2145–2150
58. Gertz K, Kronenberg G, Kälin RE, Baldinger T, Werner C, Balkaya M, Eom GD, Hellmann-Regen J et al (2012) Essential role of interleukin-6 in post-stroke angiogenesis. Brain. 135:1964–1980
59. Hoffmann CJ, Harms U, Rex A, Szulzewsky F, Wolf SA, Grittner U et al (2015) Vascular signal transducer and activator of transcription-3 promotes angiogenesis and neuroplasticity long-term after stroke. Circulation. 131:1772–1782
60. Horie N, Pereira MP, Niizuma K, Sun G, Keren-Gill H, Encarnacion A, Shamloo M, Hamilton SA et al (2011) Transplanted stem cell-secreted vascular endothelial growth factor effects poststroke recovery, inflammation, and vascular repair. Stem Cells 29:274–285
61. Manoonkitiwongsa PS, Jackson-Friedman C, McMillan PJ, Schultz RL, Lyden PD (2001) Angiogenesis after stroke is correlated with increased numbers of macrophages: the clean-up hypothesis. J Cereb Blood Flow Metab 21:1223–1231
62. Gertz K, Kronenberg G, Uhlemann R, Prinz V, Marquina R, Corada M et al (2016) Partial loss of VE-cadherin improves long-term outcome and cerebral blood flow after transient brain ischemia in mice. BMC Neurol 16:144
63. Gertz K, Priller J, Kronenberg G, Fink KB, Winter B, Schröck H et al (2006) Physical activity improves long-term stroke outcome via endothelial nitric oxide synthase-dependent augmentation of neovascularization and cerebral blood flow. Circ Res 99:1132–1140
64. Boon RA, Iekushi K, Lechner S, Seeger T, Fischer A, Heydt S, Kaluza D, Tréguer K et al (2013) MicroRNA-34a regulates cardiac ageing and function. Nature. 495:107–110
65. Yang Y, Cheng H-W, Qiu Y, Dupee D, Noonan M, Lin Y-D et al (2015) MicroRNA-34a plays a key role in cardiac repair and regeneration following myocardial infarction. Circ Res 117:450–459
66. Hattori Y, Okamoto Y, Maki T, Yamamoto Y, Oishi N, Yamahara K, Nagatsuka K, Takahashi R et al (2014) Silent information regulator 2 homolog 1 counters cerebral hypoperfusion injury by deacetylating endothelial nitric oxide synthase. Stroke. 45:3403–3411
67. Wan Y, Liu Y, Wang X, Wu J, Liu K, Zhou J et al (2015) Identification of differential microRNAs in cerebrospinal fluid and serum of patients with major depressive disorder. PLoS One 10:e0121975
68. Bavamian S, Mellios N, Lalonde J, Fass DM, Wang J, Sheridan SD, Madison JM, Zhou F et al (2015) Dysregulation of miR-34a links neuronal development to genetic risk factors for bipolar disorder. Mol Psychiatry 20:573–584
69. Su W, Hopkins S, Nesser NK, Sopher B, Silvestroni A, Ammanuel S et al (2014) The p53 transcription factor modulates microglia behavior through microRNA-dependent regulation of c-Maf. J Immunol 192:358–366

# Supplementary Material

Molecular Neurobiology

## Endothelial Cell-Specific Transcriptome Reveals Signature of Chronic Stress Related to Worse Outcome After Mild Transient Brain Ischemia in Mice

Stephanie Wegner, M.Sc.[1], Ria Uhlemann, Ph.D.[1], Valérie Boujon, M.Sc.[1], Burcu Ersoy, M.Sc.[1], Matthias Endres, M.D.[1,2,3], Golo Kronenberg, M.D.[1,4]*, Karen Gertz, M.D.[1,2]*

* These authors contributed equally to this work.

1. Klinik für Neurologie, Charité Campus Mitte, Charité - Universitätsmedizin Berlin, Charitéplatz 1, 10117 Berlin, Germany
2. DZHK (German Center for Cardiovascular Research), Partner site Berlin, 10115 Berlin, Germany
3. Deutsches Zentrum für Neurodegenerative Erkrankungen (DZNE), 10117 Berlin, Germany
4. University of Leicester and Leicestershire Partnership NHS Trust, Leicester, United Kingdom

**ESM 1**

GO enrichment analysis of differentially expressed genes. **a.** Complete list of biological process GO terms enriched in both groups. **b.** Complete list of biological process GO terms which were only found to be significantly enriched in CS samples. **c.** Complete list of biological process GO terms enriched exclusively in samples derived from C mice. C, Control. CS, Chronic stress

**ESM 2**

DEGs that emerged in ECs from both control (C) and chronically stressed (CS) mice

**ESM 3**

DEGs that were only detected in ECs from C mice

**ESM 4**

DEGs that were only detected in ECs from CS mice

**ESM1**

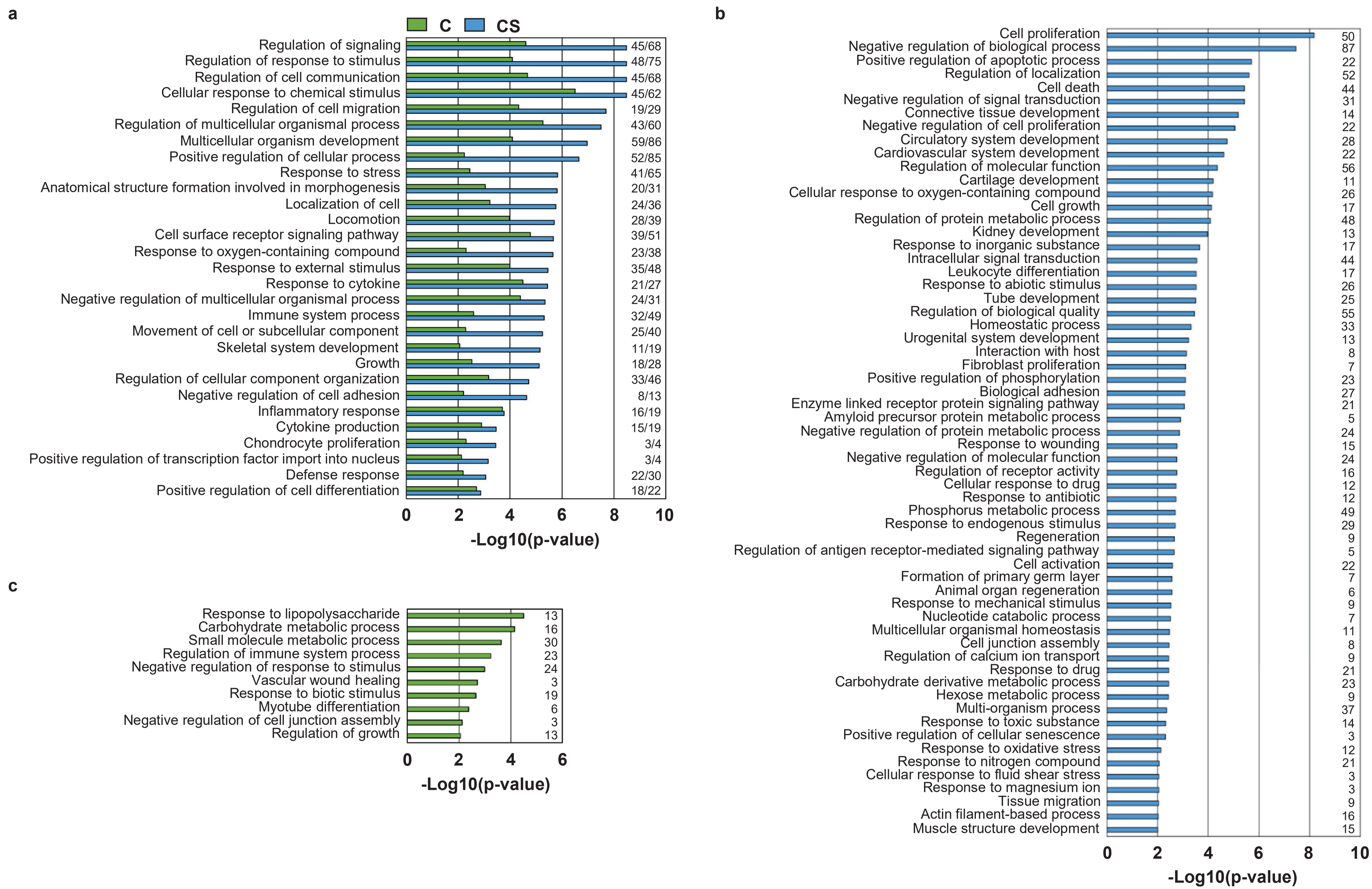

a
C
CS
Regulation of signaling 45/68
Regulation of response to stimulus 48/75
Regulation of cell communication 45/68
Cellular response to chemical stimulus 45/62
Regulation of cell migration 19/29
Regulation of multicellular organismal process 43/60
Multicellular organism development 59/86
Positive regulation of cellular process 52/85
Response to stress 41/65
Anatomical structure formation involved in morphogenesis 20/31
Localization of cell 24/36
Locomotion 28/39
Cell surface receptor signaling pathway 39/51
Response to oxygen-containing compound 23/38
Response to external stimulus 35/48
Response to cytokine 21/27
Negative regulation of multicellular organismal process 24/31
Immune system process 32/49
Movement of cell or subcellular component 25/40
Skeletal system development 11/19
Growth 18/28
Regulation of cellular component organization 33/46
Negative regulation of cell adhesion 8/13
Inflammatory response 16/19
Cytokine production 15/19
Chondrocyte proliferation 3/4
Positive regulation of transcription factor import into nucleus 3/4
Defense response 22/30
Positive regulation of cell differentiation 18/22
0 2 4 6 8 10
-Log10(p-value)
b
Cell proliferation 50
Negative regulation of biological process 87
Positive regulation of apoptotic process 22
Regulation of localization 52
Cell death 44
Negative regulation of signal transduction 31
Connective tissue development 14
Negative regulation of cell proliferation 22
Circulatory system development 28
Cardiovascular system development 22
Regulation of molecular function 56
Cartilage development 11
Cellular response to oxygen-containing compound 26
Cell growth 17
Regulation of protein metabolic process 48
Kidney development 13
Response to inorganic substance 17
Intracellular signal transduction 44
Leukocyte differentiation 17
Response to abiotic stimulus 26
Tube development 25
Regulation of biological quality 55
Homeostatic process 33
Urogenital system development 13
Interaction with host 8
Fibroblast proliferation 7
Positive regulation of phosphorylation 23
Biological adhesion 27
Enzyme linked receptor protein signaling pathway 21
Amyloid precursor protein metabolic process 5
Negative regulation of protein metabolic process 24
Response to wounding 15
Negative regulation of molecular function 24
Regulation of receptor activity 16
Cellular response to drug 12
Response to antibiotic 12
Phosphorus metabolic process 49
Response to endogenous stimulus 29
Regeneration 9
Regulation of antigen receptor-mediated signaling pathway 5
Cell activation 22
Formation of primary germ layer 7
Animal organ regeneration 6
Response to mechanical stimulus 9
Nucleotide catabolic process 7
Multicellular organismal homeostasis 11
Cell junction assembly 8
Regulation of calcium ion transport 9
Response to drug 21
Carbohydrate derivative metabolic process 23
Hexose metabolic process 9
Multi-organism process 37
Response to toxic substance 14
Positive regulation of cellular senescence 3
Response to oxidative stress 12
Response to nitrogen compound 21
Cellular response to fluid shear stress 3
Response to magnesium ion 3
Tissue migration 9
Actin filament-based process 16
Muscle structure development 15
0 2 4 6 8 10
-Log10(p-value)
c
Response to lipopolysaccharide 13
Carbohydrate metabolic process 16
Small molecule metabolic process 30
Regulation of immune system process 23
Negative regulation of response to stimulus 24
Vascular wound healing 3
Response to biotic stimulus 19
Myotube differentiation 6
Negative regulation of cell junction assembly 3
Regulation of growth 13
0 2 4 6
-Log10(p-value)

**ESM 2** DEGs that emerged in ECs from both control (C) and chronically stressed (CS) mice

| No | Gene | Log2(fold change)_C | FDR_C | Log2(fold change)_CS | FDR_CS | DE |
|---|---|---|---|---|---|---|
| **1** | *Itih4* | 5.85 | 0.006 | 2.30 | 0.021 | Up |
| **2** | *AA467197* | 4.26 | 0.006 | 3.58 | 0.003 | Up |
| **3** | *Lrg1* | 3.24 | 0.006 | 2.70 | 0.003 | Up |
| **4** | *Apod* | 3.07 | 0.006 | 2.02 | 0.003 | Up |
| **5** | *Scgb3a1* | 2.94 | 0.006 | 2.36 | 0.003 | Up |
| **6** | *Pdlim1* | 2.93 | 0.006 | 3.46 | 0.003 | Up |
| **7** | *Fbp1* | 2.81 | 0.006 | 3.11 | 0.003 | Up |
| **8** | *Csf2rb* | 2.78 | 0.006 | 2.56 | 0.003 | Up |
| **9** | *Igfbp6* | 2.78 | 0.011 | 3.10 | 0.021 | Up |
| **10** | *4933407L21Rik* | 2.75 | 0.034 | 3.09 | 0.034 | Up |
| **11** | *Ctsw* | 2.59 | 0.006 | 1.63 | 0.003 | Up |
| **12** | *Dusp2* | 2.58 | 0.006 | 2.15 | 0.003 | Up |
| **13** | *Serpine1* | 2.50 | 0.031 | 2.05 | 0.017 | Up |
| **14** | *Dok3* | 2.43 | 0.006 | 1.75 | 0.003 | Up |
| **15** | *Chst1* | 2.43 | 0.006 | 2.88 | 0.003 | Up |
| **16** | *Gpr55* | 2.38 | 0.025 | 1.98 | 0.003 | Up |
| **17** | *Ace* | 2.30 | 0.006 | 1.60 | 0.003 | Up |
| **18** | *Upp1* | 2.23 | 0.006 | 2.87 | 0.003 | Up |
| **19** | *Atp8b1* | 2.23 | 0.006 | 2.01 | 0.003 | Up |
| **20** | *Rnf183* | 2.23 | 0.006 | 2.60 | 0.003 | Up |
| **21** | *Tmem173* | 2.21 | 0.006 | 2.15 | 0.003 | Up |
| **22** | *Tnfsf8* | 2.21 | 0.006 | 2.10 | 0.003 | Up |
| **23** | *Cpe* | 2.16 | 0.006 | 1.48 | 0.003 | Up |
| **24** | *Lgmn* | 2.11 | 0.006 | 1.81 | 0.003 | Up |
| **25** | *Igfbp4* | 2.10 | 0.006 | 2.00 | 0.003 | Up |
| **26** | *Oaf* | 2.08 | 0.028 | 2.51 | 0.003 | Up |
| **27** | *Bmp4* | 2.05 | 0.006 | 2.01 | 0.003 | Up |
| **28** | *Myc* | 2.05 | 0.006 | 2.28 | 0.003 | Up |
| **29** | *Trp53i11* | 2.02 | 0.006 | 2.56 | 0.003 | Up |
| **30** | *Cd14* | 1.94 | 0.006 | 2.90 | 0.003 | Up |
| **31** | *Best1* | 1.92 | 0.006 | 1.81 | 0.003 | Up |
| **32** | *Lao1* | 1.88 | 0.006 | 1.56 | 0.003 | Up |
| **33** | *Dbn1* | 1.79 | 0.006 | 1.47 | 0.013 | Up |
| **34** | *Aldh3b1* | 1.79 | 0.006 | 1.92 | 0.003 | Up |
| **35** | *Spred3* | 1.79 | 0.011 | 1.43 | 0.025 | Up |
| **36** | *Inhbb* | 1.76 | 0.006 | 2.57 | 0.003 | Up |
| **37** | *Ifitm1* | 1.75 | 0.006 | 2.79 | 0.003 | Up |
| **38** | *Mmp14* | 1.74 | 0.006 | 1.45 | 0.015 | Up |
| **39** | *Sphk1* | 1.74 | 0.015 | 1.83 | 0.003 | Up |
| **40** | *Fosl1* | 1.71 | 0.006 | 2.55 | 0.003 | Up |
| **41** | *B3gnt3* | 1.67 | 0.006 | 1.20 | 0.006 | Up |
| **42** | *Gpr182* | 1.67 | 0.006 | 1.41 | 0.003 | Up |
| **43** | *Plekho2* | 1.67 | 0.006 | 1.56 | 0.003 | Up |
| **44** | *Hcls1* | 1.65 | 0.006 | 1.95 | 0.003 | Up |
| **45** | *4930486L24Rik* | 1.62 | 0.006 | 1.69 | 0.003 | Up |
| **46** | *Ppp1r14b* | 1.59 | 0.006 | 1.59 | 0.003 | Up |
| **47** | *Gmpr* | 1.59 | 0.006 | 1.62 | 0.003 | Up |
| **48** | *Tubb6* | 1.56 | 0.006 | 2.35 | 0.003 | Up |
| **49** | *Plekho1* | 1.56 | 0.006 | 1.07 | 0.041 | Up |
| **50** | *Glipr2* | 1.54 | 0.006 | 1.78 | 0.003 | Up |
| **51** | *Tmem252* | 1.54 | 0.006 | 2.16 | 0.003 | Up |
| **52** | *Synpo* | 1.53 | 0.006 | 1.68 | 0.003 | Up |
| **53** | *Ctla2b* | 1.50 | 0.006 | 1.57 | 0.003 | Up |
| **54** | *Adgrg3* | 1.49 | 0.006 | 1.05 | 0.006 | Up |
| **55** | *Hid1* | 1.48 | 0.006 | 1.20 | 0.003 | Up |
| **56** | *Mcam* | 1.47 | 0.006 | 1.25 | 0.003 | Up |
| **57** | *Snai1* | 1.43 | 0.015 | 1.34 | 0.037 | Up |
| **58** | *Acp5* | 1.41 | 0.006 | 1.35 | 0.003 | Up |
| **59** | *Slc10a6* | 1.40 | 0.006 | 1.99 | 0.003 | Up |

| No | Gene | Log2(fold change)_C | FDR_C | Log2(fold change)_CS | FDR_CS | DE |
|---|---|---|---|---|---|---|
| **60** | *Itm2c* | 1.38 | 0.006 | 1.41 | 0.003 | Up |
| **61** | *Ecscr* | 1.38 | 0.006 | 1.55 | 0.003 | Up |
| **62** | *Mustn1* | 1.38 | 0.006 | 1.30 | 0.003 | Up |
| **63** | *Marcksl1* | 1.36 | 0.006 | 1.89 | 0.003 | Up |
| **64** | *Ch25h* | 1.35 | 0.006 | 1.75 | 0.003 | Up |
| **65** | *Xbp1* | 1.34 | 0.006 | 1.17 | 0.003 | Up |
| **66** | *C1qtnf6* | 1.32 | 0.028 | 1.91 | 0.003 | Up |
| **67** | *BC018473* | 1.25 | 0.011 | 1.69 | 0.003 | Up |
| **68** | *Uchl3* | 1.22 | 0.006 | 1.22 | 0.003 | Up |
| **69** | *Pde4b* | 1.21 | 0.006 | 1.52 | 0.003 | Up |
| **70** | *Smim3* | 1.21 | 0.006 | 1.47 | 0.003 | Up |
| **71** | *Prr5* | 1.21 | 0.050 | 1.59 | 0.003 | Up |
| **72** | *Zfp521* | 1.19 | 0.006 | 1.06 | 0.003 | Up |
| **73** | *Rplp0* | 1.19 | 0.006 | 1.04 | 0.003 | Up |
| **74** | *Dnah6* | 1.19 | 0.006 | 1.32 | 0.003 | Up |
| **75** | *Hilpda* | 1.19 | 0.006 | 1.15 | 0.003 | Up |
| **76** | *Htra3* | 1.16 | 0.006 | 1.08 | 0.003 | Up |
| **77** | *Gm9625* | 1.16 | 0.006 | 1.14 | 0.003 | Up |
| **78** | *Adm* | 1.16 | 0.006 | 1.74 | 0.003 | Up |
| **79** | *Gm8730* | 1.16 | 0.006 | 1.08 | 0.003 | Up |
| **80** | *Apln* | 1.11 | 0.028 | 3.47 | 0.003 | Up |
| **81** | *Eva1a* | 1.10 | 0.006 | 1.11 | 0.003 | Up |
| **82** | *Plp2* | 1.08 | 0.006 | 1.22 | 0.003 | Up |
| **83** | *Ptpre* | 1.07 | 0.006 | 1.81 | 0.003 | Up |
| **84** | *Slc16a3* | 1.03 | 0.015 | 1.43 | 0.003 | Up |
| **85** | *Arrdc3* | 1.02 | 0.011 | 1.26 | 0.003 | Up |
| **86** | *Cmtm3* | 1.01 | 0.006 | 1.14 | 0.003 | Up |
| **87** | *Tnfrsf1a* | 1.01 | 0.006 | 1.00 | 0.003 | Up |
| **88** | *Pawr* | 1.01 | 0.022 | 1.05 | 0.003 | Up |
| **89** | *Il18bp* | 1.00 | 0.011 | 1.10 | 0.003 | Up |
| **90** | *Nov* | -2.08 | 0.006 | -2.40 | 0.003 | Down |
| **91** | *Slc26a10* | -1.46 | 0.006 | -1.10 | 0.003 | Down |
| **92** | *Klf15* | -1.30 | 0.022 | -2.01 | 0.003 | Down |
| **93** | *Pi16* | -1.14 | 0.006 | -1.02 | 0.003 | Down |

DE = differentially expressed

**ESM 3** DEGs that were only detected in ECs from C mice

| No | Gene | Log2(fold change) | FDR | DE |
|---|---|---|---|---|
| 1 | *Wisp2* | 3.96 | 0.019 | Up |
| 2 | *2810459M11Rik* | 2.07 | 0.046 | Up |
| 3 | *Csf2rb2* | 1.78 | 0.006 | Up |
| 4 | *Plxnb2* | 1.55 | 0.006 | Up |
| 5 | *Abca1* | 1.49 | 0.006 | Up |
| 6 | *Steap3* | 1.37 | 0.006 | Up |
| 7 | *Lbp* | 1.25 | 0.011 | Up |
| 8 | *Ptgfrn* | 1.22 | 0.006 | Up |
| 9 | *Il20rb* | 1.21 | 0.006 | Up |
| 10 | *Scn1b* | 1.19 | 0.006 | Up |
| 11 | *Gadd45b* | 1.18 | 0.006 | Up |
| 12 | *Itpr3* | 1.14 | 0.006 | Up |
| 13 | *2410006H16Rik* | 1.13 | 0.019 | Up |
| 14 | *Fam43a* | 1.11 | 0.006 | Up |
| 15 | *Bcr* | 1.11 | 0.006 | Up |
| 16 | *Nid1* | 1.11 | 0.006 | Up |
| 17 | *Slco2b1* | 1.09 | 0.006 | Up |
| 18 | *Il4ra* | 1.07 | 0.006 | Up |
| 19 | *Socs3* | 1.06 | 0.006 | Up |
| 20 | *Spns2* | 1.04 | 0.028 | Up |
| 21 | *Gm6472* | 1.04 | 0.006 | Up |
| 22 | *Gm15500* | 1.03 | 0.022 | Up |
| 23 | *Rps11* | 1.02 | 0.006 | Up |
| 24 | *Pdia5* | 1.01 | 0.006 | Up |
| 25 | *Chst7* | 1.01 | 0.022 | Up |
| 26 | *Adgrb1* | -7.92 | 0.006 | Down |
| 27 | *Gm27357,Gm27627,Gm27882,Gm27998,Miat* | -4.14 | 0.006 | Down |
| 28 | *Gm27718,Gm27913,Gm27957,Pvt1* | -3.92 | 0.006 | Down |
| 29 | *DQ267100,Gm23508,Gm24895,Gm26922,Gm27350,Rian* | -3.61 | 0.006 | Down |
| 30 | *Psd4* | -3.57 | 0.006 | Down |
| 31 | *4833445I07Rik* | -3.15 | 0.006 | Down |
| 32 | *Sema4a* | -2.89 | 0.006 | Down |
| 33 | *Bcat1* | -2.72 | 0.031 | Down |
| 34 | *Catsperg2* | -2.68 | 0.015 | Down |
| 35 | *Jakmip1* | -2.67 | 0.006 | Down |
| 36 | *Gm27875,Jpx* | -2.45 | 0.022 | Down |
| 37 | *Lemd1* | -2.45 | 0.048 | Down |
| 38 | *Trpm1* | -2.41 | 0.011 | Down |
| 39 | *Pappa2* | -2.30 | 0.037 | Down |
| 40 | *Gm16503* | -2.20 | 0.015 | Down |
| 41 | *Elavl2* | -2.06 | 0.015 | Down |
| 42 | *Agxt2,Gm21973,Prlr* | -2.04 | 0.006 | Down |
| 43 | *Dlgap1* | -1.72 | 0.011 | Down |
| 44 | *Map2* | -1.65 | 0.011 | Down |
| 45 | *Gm13034* | -1.65 | 0.040 | Down |
| 46 | *Ugt1a1,Ugt1a10,Ugt1a2,Ugt1a5,Ugt1a6a,Ugt1a6b,Ugt1a7c,Ugt1a8,Ugt1a9* | -1.63 | 0.006 | Down |
| 47 | *Maf* | -1.50 | 0.048 | Down |
| 48 | *Adam22* | -1.48 | 0.006 | Down |
| 49 | *Arpp21* | -1.47 | 0.019 | Down |
| 50 | *Meis2* | -1.46 | 0.048 | Down |
| 51 | *Ubn2* | -1.46 | 0.006 | Down |
| 52 | *Ptprd* | -1.36 | 0.034 | Down |
| 53 | *Eif3j2* | -1.36 | 0.006 | Down |
| 54 | *Acta2* | -1.08 | 0.015 | Down |
| 55 | *Alpl* | -1.04 | 0.006 | Down |
| 56 | *Gm9946* | -1.04 | 0.046 | Down |

DE = differentially expressed

**ESM 4** DEGs that were only detected in ECs from CS mice

| No | Gene | Log2(fold change) | FDR | DE |
|---|---|---|---|---|
| 1 | *Gm5134* | 4.83 | 0.042 | Up |
| 2 | *Kcne3* | 4.07 | 0.003 | Up |
| 3 | *Gm37795,Mir34a* | 3.40 | 0.040 | Up |
| 4 | *Rnf225* | 3.02 | 0.009 | Up |
| 5 | *Ackr1,Cadm3* | 3.00 | 0.003 | Up |
| 6 | *Csf3* | 2.77 | 0.003 | Up |
| 7 | *Pgf* | 2.77 | 0.003 | Up |
| 8 | *Ctla2a* | 2.22 | 0.003 | Up |
| 9 | *Kif17,Sh2d5* | 2.16 | 0.003 | Up |
| 10 | *Fscn1* | 2.11 | 0.003 | Up |
| 11 | *Cda* | 2.04 | 0.023 | Up |
| 12 | *Mdfi* | 2.04 | 0.003 | Up |
| 13 | *Lyve1* | 2.01 | 0.003 | Up |
| 14 | *Fbp2* | 1.98 | 0.034 | Up |
| 15 | *Odc1* | 1.96 | 0.003 | Up |
| 16 | *Psors1c2* | 1.94 | 0.006 | Up |
| 17 | *Rab20* | 1.94 | 0.003 | Up |
| 18 | *Car13* | 1.90 | 0.046 | Up |
| 19 | *C1qtnf5,Mfrp* | 1.90 | 0.009 | Up |
| 20 | *Cxcl16* | 1.71 | 0.003 | Up |
| 21 | *Hmga1* | 1.68 | 0.015 | Up |
| 22 | *Plpp2* | 1.66 | 0.003 | Up |
| 23 | *Angpt2* | 1.65 | 0.009 | Up |
| 24 | *Kit* | 1.65 | 0.003 | Up |
| 25 | *Gm7993* | 1.61 | 0.006 | Up |
| 26 | *Lgals3* | 1.61 | 0.003 | Up |
| 27 | *Pycr1* | 1.60 | 0.031 | Up |
| 28 | *Mt2* | 1.60 | 0.003 | Up |
| 29 | *Acot7* | 1.55 | 0.003 | Up |
| 30 | *Adamts9* | 1.50 | 0.047 | Up |
| 31 | *Slc16a6* | 1.49 | 0.042 | Up |
| 32 | *Kcnj15* | 1.48 | 0.026 | Up |
| 33 | *Fkbp1a* | 1.47 | 0.003 | Up |
| 34 | *Itgb3* | 1.46 | 0.006 | Up |
| 35 | *Ccnd1* | 1.45 | 0.003 | Up |
| 36 | *Nt5e* | 1.42 | 0.033 | Up |
| 37 | *Frzb* | 1.41 | 0.048 | Up |
| 38 | *Osgin1* | 1.36 | 0.003 | Up |
| 39 | *Cd82* | 1.32 | 0.003 | Up |
| 40 | *Hmga1-rs1* | 1.30 | 0.003 | Up |
| 41 | *Gale* | 1.30 | 0.003 | Up |
| 42 | *Sdcbp2* | 1.29 | 0.003 | Up |
| 43 | *Spp1* | 1.29 | 0.003 | Up |
| 44 | *Kcnj8* | 1.28 | 0.003 | Up |
| 45 | *Tfpi2* | 1.26 | 0.036 | Up |
| 46 | *Mt1* | 1.26 | 0.006 | Up |
| 47 | *Meox1* | 1.22 | 0.003 | Up |
| 48 | *Tuba1c* | 1.21 | 0.003 | Up |
| 49 | *Tnfrsf10b* | 1.21 | 0.003 | Up |
| 50 | *Stx11* | 1.21 | 0.003 | Up |
| 51 | *Nectin2* | 1.21 | 0.017 | Up |
| 52 | *Litaf* | 1.20 | 0.003 | Up |
| 53 | *Plaur* | 1.19 | 0.003 | Up |
| 54 | *S100a6* | 1.18 | 0.003 | Up |
| 55 | *Lgals1* | 1.18 | 0.039 | Up |
| 56 | *Map1b* | 1.17 | 0.003 | Up |
| 57 | *Rnd1* | 1.17 | 0.003 | Up |
| 58 | *Crlf2* | 1.17 | 0.003 | Up |
| 59 | *Abi3* | 1.16 | 0.033 | Up |

| No | Gene | Log2(fold change) | FDR | DE |
|---|---|---|---|---|
| **60** | *Serpinh1* | 1.15 | 0.003 | Up |
| **61** | *Gm20489,Gm614,Il2rg* | 1.13 | 0.003 | Up |
| **62** | *Gm10282* | 1.12 | 0.050 | Up |
| **63** | *Ube2m* | 1.11 | 0.003 | Up |
| **64** | *Phlda1* | 1.11 | 0.003 | Up |
| **65** | *Emp1* | 1.10 | 0.003 | Up |
| **66** | *Eif4ebp1* | 1.09 | 0.003 | Up |
| **67** | *Nrarp* | 1.08 | 0.003 | Up |
| **68** | *Hmgn2* | 1.07 | 0.006 | Up |
| **69** | *Ifitm3* | 1.07 | 0.003 | Up |
| **70** | *Smad1* | 1.06 | 0.003 | Up |
| **71** | *Gapdh* | 1.05 | 0.013 | Up |
| **72** | *Kctd17* | 1.05 | 0.003 | Up |
| **73** | *Ubtd1* | 1.05 | 0.003 | Up |
| **74** | *Ppa1* | 1.04 | 0.003 | Up |
| **75** | *Nrgn* | 1.03 | 0.046 | Up |
| **76** | *Hmox1* | 1.03 | 0.003 | Up |
| **77** | *Pdia6* | 1.03 | 0.003 | Up |
| **78** | *Stc1* | 1.03 | 0.013 | Up |
| **79** | *Ctsb* | 1.02 | 0.003 | Up |
| **80** | *Timeless* | 1.02 | 0.003 | Up |
| **81** | *Tcf19* | 1.02 | 0.003 | Up |
| **82** | *Sh3bp5* | 1.01 | 0.003 | Up |
| **83** | *Sod3* | 1.01 | 0.028 | Up |
| **84** | *5031439G07Rik* | 1.00 | 0.003 | Up |
| **85** | *Mall* | 1.00 | 0.003 | Up |
| **86** | *Spry4* | 1.00 | 0.003 | Up |
| **87** | *Lrrc32* | 1.00 | 0.003 | Up |
| **88** | *Gm28045,Prnd,Prnp* | 1.00 | 0.011 | Up |
| **89** | *Rttn* | -4.91 | 0.003 | Down |
| **90** | *Pm20d1* | -4.45 | 0.003 | Down |
| **91** | *Gria2* | -3.19 | 0.003 | Down |
| **92** | *Ptpn6* | -2.65 | 0.039 | Down |
| **93** | *Wnt11* | -2.24 | 0.041 | Down |
| **94** | *Plch2* | -2.18 | 0.031 | Down |
| **95** | *Dock7* | -1.68 | 0.003 | Down |
| **96** | *Doc2b* | -1.68 | 0.003 | Down |
| **97** | *B4galnt1* | -1.48 | 0.006 | Down |
| **98** | *Vwa3a* | -1.47 | 0.011 | Down |
| **99** | *Fgfr3* | -1.46 | 0.003 | Down |
| **100** | *Trp53inp1* | -1.43 | 0.003 | Down |
| **101** | *Nr4a1* | -1.43 | 0.003 | Down |
| **102** | *Exoc3l2* | -1.41 | 0.003 | Down |
| **103** | *Tmcc2* | -1.33 | 0.003 | Down |
| **104** | *Kank4* | -1.19 | 0.003 | Down |
| **105** | *Lamc3* | -1.15 | 0.003 | Down |
| **106** | *Acacb* | -1.13 | 0.003 | Down |
| **107** | *Cyp26b1* | -1.11 | 0.003 | Down |
| **108** | *Cytl1* | -1.10 | 0.003 | Down |
| **109** | *Nog* | -1.09 | 0.003 | Down |
| **110** | *Tprn* | -1.06 | 0.003 | Down |
| **111** | *Mycl* | -1.03 | 0.037 | Down |
| **112** | *Palm* | -1.02 | 0.003 | Down |
| **113** | *Pmaip1* | -1.02 | 0.003 | Down |
| **114** | *Trpv4* | -1.00 | 0.003 | Down |

DE = differentially expressed

## Curriculum vitae

My curriculum vitae is not included in the online version due to data protection reasons.

## List of publications

Impact factors (IF) are taken from Web of Science, Journal Summary List 2017.

Endothelial cell-specific transcriptome reveals signature of chronic stress related to worse outcome after mild transient brain ischemia in mice.

**Wegner S**, Uhlemann R, Boujon V, Ersoy B, Endres M, Kronenberg G*, Gertz K*.

Mol Neurobiol. 2020;57(3):1446-1458 **IF: 5.076**

*Authors contributed equally

Dual PPARα/γ agonist aleglitazar confers stroke protection in a model of mild focal brain ischemia in mice.

Boujon V, Uhlemann R, **Wegner S**, Wright MB, Laufs U, Endres M, Kronenberg G*, Gertz K*.

J Mol Med (Berl). 2019;97(8):1127-1138 **IF: 4.938**

* Authors contributed equally

Distinguishing features of microglia- and monocyte-derived macrophages after stroke.

Kronenberg G, Uhlemann R, Richter N, Klempin F, **Wegner S**, Staerck L, Wolf S, Uckert W, Kettenmann H, Endres M, Gertz K.

Acta Neuropathol. 2018;135(4):551-568 **IF: 15.872**

Repression of telomere-associated genes by microglia activation in neuropsychiatric disease.

Kronenberg G*, Uhlemann R*, Schöner J, **Wegner S**, Boujon V, Deigendesch N, Endres M, Gertz K.

Eur Arch Psychiatry Clin Neurosci. 2017;267(5):473-477 **IF: 3.617**

* Authors contributed equally

## Acknowledgements

With utmost respect, I would like to thank all the people who have supported me during my time at the Charité - Universitätsmedizin Berlin.

First and foremost, tremendous thanks goes to Prof. Dr. Matthias Endres for affording me the opportunity to work in his group and allowing me to expand my skills and expertise. Many thanks also to the director of the Department of Experimental Neurology, Prof. Dr. Ulrich Dirnagl, for providing a valuable research infrastructure.

I would also like to thank my supervisors PD Dr. Karen Gertz and Prof. Dr. Golo Kronenberg for their time, support, and inputs. Without their guidance and support, it would have been impossible for me to achieve my results during my tenure as PhD student.

Sincere thanks to Dr. Ria Uhlemann for being involved with me in many scientific discussions and for proofreading my thesis. I was extraordinarily fortunate to have her as a trusted teammate in the lab and for lending her support to me.

My special thanks to Melanie Kroh, Bettina Herrmann, Stefanie Balz, and Renate Franke for providing me excellent technical support throughout all my projects. I would also like to thank Jenny Kirsch from the German Rheumatism Research Center Berlin (DRFZ) for her help with the FAC-sorting of the brain endothelial cells. Also, I want to thank Dr. Diana Busch and Martin Farricker for proofreading my thesis and Burcu Ersoy for helping me with the stress experiments.

My heartfelt thanks goes also to the members of the Department of Experimental Neurology. Among them, special recognition goes to Ingo Przesdzing for numerous discussions about flow cytometry experimental setups and his problem solving skills with our FACS machine. I would also thank Susanne Müller and Dr. Philipp Böhm-Sturm for their technical support with the small animal MRI.

Last, but not least, my appreciation goes to my parents, Renate and Andreas, and my brother Sebastian, for their unwavering support and the faith in me. A special thanks to Zain for his support and patience over the years.